groups. Zonisamide monotherapy demonstrated less frequent adverse effects than zonisamide combined therapy. Combined antiepilepsy therapy often induces adverse effects more frequently in any antiepilepsy drug, not only zonisamide.[7]

In the treatment of epileptic children with zonisamide, anhidrosis accompanied by elevated body temperature has been reported, especially during summer.[8,9] Moreover, Shimizu et al. reported a case of an intellectually disabled 2-year-old boy demonstrating a heat stroke-like episode associated with zonisamide treatment.[10] This patient showed hyperpyrexia and oligohidrosis. In the present study, cases with anhidrosis were not reported by the doctors. However, anhidrosis or oligohidrosis is often difficult to observe, especially by intellectually disabled patients. Hyperpyrexia and oligohidrosis should be carefully monitored during zonisamide treatment.

References

1. Seino M, Ohkuma T, Miyasaka M, et al. Evaluation of the drug efficacy of AD-810 (zonisamide). Results of double-blind study in comparison with carbamazepine (in Japanese). *J Clin Exp Med* 1988;144:275–91.
2. Schmidt D, Jacob R, Loiseau P, et al. Zonisamide for add-on treatment of refractory partial epilepsy: a European double-blind trial. *Epilepsy Res* 1993;15:67–73.
3. Wilder BJ, Ramsay RE, Browney T, Sackellares JC. A multicenter double-blind, placebo controlled study on zonisamide on medically refractory patients with complex seizures. *Epilepsia* 1985;26:545.
4. Oguni H, Hayashi K, Fukuyama Y, Iinuma K. Phase III study of a new antiepilepsy AD-810, zonisamide in childhood epilepsy (in Japanese). *Jpn J Pediatr* 1988;41:439–50.
5. Yamatogi Y, Ohtahara S. Current topics of treatment. In: Ohtahara S, Roger J, editors. *New trends in pediatric epileptology*. 1991. p. 136–48.
6. Iinuma K, Handa I, Fueki N, Yamamoto K, Kojima A, Haginoya K. Effects of zonisamide (AD-810) on refractory epilepsy in children: special reference to temporal lobe abnormalities. *Curr Ther Res* 1988;43:281–90.
7. Guberman A. Monotherapy or polytherapy for epilepsy? *Can J Neurol Sci* 1998;25:53–8.
8. Fujita Y, Okubo O, Noguchi Y, Nishimura A, Fuchigami T, Harada K. Zonisamide-induced hidropoietic disorder in patients with childhood epilepsy. *J Nihon Univ Med Assoc* 1995;54:658–62.
9. Okumura A, Hayakawa F, Kuno K, Watanabe K. Oligohidrosis caused by zonisamide. *No To Hattatsu* 1996;28:44–7 (in Japanese).
10. Shimizu T, Yamashita Y, Satoi M, et al. Heat stroke-like episode in a child caused by zonisamide. *Brain Dev* 1997;19:366–8.

Should thrombolysis be given to a stroke patient refusing therapy due to profound anosognosia?

Jeffrey M. Katz, MD; and Alan Z. Segal, MD

A 70-year-old woman was told by a neighbor that her speech was slurred. She was also having difficulty standing. She was brought to the emergency room within 45 minutes of symptom onset stating "they said I had a stroke, but I didn't." She had a history of hypertension, hypercholesterolemia, and stage IV non-small cell lung cancer. Her examination was notable for a severe anosognosia, dysarthria, a right gaze preference, and left homonymous hemianopia, hemiparesis, hemihypesthesia, and visual, tactile, and spatial neglect. Her NIH Stroke Scale score was 15. Head CT was unremarkable, and she had no contraindications for IV thrombolysis.

Preparations were made for the administration of tPA, at approximately 2 hours after symptom onset. The patient, however, vehemently refused therapy because she did not believe she was having a stroke. Attempts were made to contact the patient's family, but this did not prove possible until after the 3-hour time window had elapsed. Upon discharge to our acute rehabilitation facility, the patient required maximal assist for transfers, remained hemiparetic, and had persistent neglect and hemianopia.

Although the administration of tPA does not require written informed consent, the risks and benefits of this therapy must be explained to the patient and family to the greatest extent possible.[1] According to the American Academy of Neurology (AAN) position paper,[2] tPA may be given without consent, if considered an accepted standard of care, in keeping with the doctrine of emergency treatment and implied consent. This would apply in particular to patients who are unable to speak due to acute aphasia. Our patient differs in that she was interactive and talkative, and was actively refusing to be treated. Because her anosognosia prevented her from properly comprehending the nature of her medical situation, she was only partially competent to make this decision.[3] Her lack of complete competency, however, still may not warrant treating her against her will. tPA has long-term benefits but also carries a trade-off of short term risk (including potentially fatal intracerebral hemorrhage). Under the pressure of a tense emergency situation, some patients may not be willing to accept this risk even without anosognosia complicating the discussion.

Since up to half of all stroke cases might involve a portion of the right middle cerebral artery and produce a component of anosognosia, we would hypothesize that our case is not entirely unusual. In an effort to expand the number of patients eligible for tPA, while ensuring compliance with valid informed consent, we would propose that the AAN consider updating its guidelines to incorporate anosognosia.

From the Department of Neurology and Neuroscience, New York Presbyterian Hospital–Weill Medical Center of Cornell University, NY.

Received May 21, 2004. Accepted in final form July 19, 2004.

Address correspondence and reprint requests to Dr. Jeffrey M. Katz, Department of Neurology and Neuroscience, New York Presbyterian Hospital–Weill Medical Center of Cornell University, 520 East 68th Street, F-610, New York, NY 10021; e-mail: drjmk@yahoo.com

References

1. Fleck LM, Hayes OW. Ethics and consent to treat issues in acute stroke therapy. Emerg Med Clin North Am 2002;20:703–715.
2. American Academy of Neurology. Consent issues in the management of cerebrovascular diseases. A position paper of the American Academy of Neurology Ethics and Humanities Subcommittee. Neurology 1999;53: 9–11.
3. Ethical practice. In: Bernat JL. Ethical issues in neurology, 2nd ed. Butterworth-Heinemann, 2002;27–49.

CSF hypocretin-1 (orexin-A) levels in childhood narcolepsy and neurologic disorders

J. Arii, MD; T. Kanbayashi, MD; Y. Tanabe, MD; Y. Sawaishi, MD; S. Kimura, MD; A. Watanabe, MD; K. Mishima, MD; Y. Hishikawa, MD; T. Shimizu, MD; and S. Nishino, MD, PhD

Hypersomnia and cataplexy expression in childhood narcolepsy are often different from adult cases, making diagnosis difficult.[1] The Multiple Sleep Latency Test (MSLT) for demonstrating hypersomnia and sleep-onset REM periods has not been standardized for children under age 8[2] and has limited value in pediatrics.

CSF hypocretin-1 measurements were established as a new diagnostic tool for narcolepsy–cataplexy in adults[3-5] but has not yet been evaluated in children.[4] We measured CSF hypocretin-1 levels in 132 children with various neurologic disorders (including six narcoleptic children) to evaluate the diagnostic value of CSF hypocretin measures for childhood narcolepsy.

Patients and methods. We analyzed previously collected data, gathered from 1992 to 2003 for diagnostic and research purposes, including CSF samples (n = 132, including 14 cases previously reported), collected from patients (under age 20 from seven Japanese hospitals) with neurologic disorders (the core experimental protocol was approved at Akita University in August 2002; the local ethical committee approved the use of CSF samples). Patients were categorized based on the diagnosis determined by individual clinical records (table). Patients without complete records or definite diagnosis were excluded. Narcolepsy was diagnosed by the criteria of the International Classification of Sleep Disorders.[6]

Hypocretin-1 was measured by direct radioimmunoassay of CSF stored at −80 °C (detection limit 40 pg/mL).[7] As there was no difference in the mean CSF hypocretin level between children and adults,[7] the levels were defined as low (<110 pg/mL), intermediate (≥110 to ≤200 pg/mL), and normal (>200 pg/mL).[5] The low value represents 30% of the mean value of normal adult CSF hypocretin and has the best sensitivity/specificity ratio for diagnosing adult narcolepsy.[5]

Results. Low CSF hypocretin-1 levels were observed in all six narcoleptic subjects (mean age 9.7 years; 6 to 16 years) (see the table; see also table E-1 on the *Neurology* Web site at www.neurology.org). All narcoleptic subjects had positive human leukocyte antigen DR2 markers. The duration of hypersomnia (DH) was 1 to 20 months prior to the CSF sampling. In two of these patients (DH: 1 and 2 months), the clinical diagnosis of narcolepsy was not clear at the time of the CSF sampling. Nevertheless, they later exhibited cataplexy, a typical symptom of narcolepsy.

In four neurologic categories, Guillain–Barré syndrome (GBS) (6/6), acute disseminated encephalomyelitis (ADEM) (2/7), brain tumor (2/4), and head trauma (3/3), 13 children had low to intermediate hypocretin-1 levels (see the table; also see table E-2 on the *Neurology* Web site).

All GBS subjects in this study showed reduced CSF hypocretin levels. Only one case (151 pg/mL) exhibited short sleep latency (<1 minute) by a two-nap test after the recovery of the neurologic symptoms. Two ADEM cases (102 and 146 pg/mL) presented transient sleepiness associated with bilateral hypothalamic lesions on MRI. Two subjects with head trauma and two with brain tumor reported sleepiness, and these subjects together with one subject with head trauma without sleepiness had reduced levels.

Intermediate hypocretin-1 levels were also found in some neuropediatric-specific conditions, such as Prader–Willi syndrome

Additional material related to this article can be found on the *Neurology* Web site. Go to www.neurology.org and scroll down the Table of Contents for the December 28 issue to find the title link for this article.

Table CSF hypocretin-1 levels in various neurologic disorders

Diagnosis	n	Low, <110 pg/mL	Intermediate, 110–200 pg/mL	Mean hypocretin-1 level (range), pg/mL
Narcolepsy (EDS with/without cataplexy, all are DR2 positive)	6	6	0	(L–79)
MSL ≦8 min + ≧2 SOREMPs	4	4	0	<40
MSL ≦8 min + no SOREMPs	2	2	0	<40, 79
Other primary hypersomnia (recurrent hypersomnia, idiopathic hypersomnia)	5	0	0	263 (232–292)
CNS infection (meningitis, encephalitis, cerebellitis)	22	0	2	282 (156–423)
Autoimmune and postinfectious disease	18	3	5	202 (L–366)
GBS	6	2	4	
ADEM	7	1	1	
Others (MS, CIDP, myelopathy)	5	0	0	
Head trauma (subdural hematoma, diffuse axonal injury, contusion)	3	1	2	132 (56–192)
Brain tumor (hypothalamic tumor, thalamic tumor)	4	1	1	175 (102–257)
Malignancy without CNS invasion (leukemia, lymphoma)	12	0	0	297 (232–364)
Psychological/psychiatric status (depression, hysteria)	3	0	0	303 (265–345)
CNS malformations (migration disorder, brain anomaly)	8	0	0	270 (223–383)
Chromosome aberration (PWS, tuberous sclerosis, Sturge–Weber syndrome)	5	0	1	233 (192–310)
Epilepsy or mental retardation of unknown origin (epilepsy, mental retardation, infantile spasms)	19	0	2	286 (124–372)
Perinatal asphyxia and trauma (cerebral palsy)	2	0	0	307 (304–310)
Metabolic or degenerative diseases (NPC, mitochondria encephalopathy, leukoencephalopathy, spinocerebellar degeneration)	6	0	1	307 (142–461)
Chronic CNS infection (SSPE)	2	0* (2)	0	313 (311–315)
Epileptic encephalopathy (progressive myoclonic encephalopathy, Lafora disease, Rasmussen encephalopathy)	3	0	0	290 (215–348)
Motor unit disease (congenital myotonic dystrophy, spinal muscular atrophy, congenital myopathy)	4	0	0	307 (265–338)
Cerebral hypertension (idiopathic cerebral hypertension, hydrocephalus)	2	0	0	320 (280–360)
Transient neurologic conditions (suspected meningitis but negative culture, migraine)	8	0	1	279 (195–338)
Total	132	11* (13)	15	

When patients received multiple CSF taps, the values during the most representative phase of the disease are reported.

* Undetectably low levels under interferon-α treatment.

L = low levels; EDS = excessive daytime sleepiness; MSL = mean sleep latency; SOREMPs = sleep-onset REM periods; GBS = Guillain–Barré syndrome; ADEM = acute disseminated encephalomyelitis; MS = multiple sclerosis; CIDP = chronic inflammatory demyelinating polyneuropathy; PWS = Prader–Willi syndrome; NPC = Niemann–Pick type C; SSPE = subacute sclerosing panencephalitis.

(PWS) (1/1), infantile spasms due to birth trauma of unknown origin (2/3), Niemann–Pick type C (NPC) (1/2), CNS infection (2/22), and febrile convulsion (1/3). None of these patients showed hypersomnia, but the NPC case with intermediate hypocretin level (147 pg/mL) presented cataplectic-like episodes.

Discussion. Five subjects in four diagnostic categories (GBS, ADEM, brain tumor, and head trauma) showed low hypocretin levels. Partial impairments of hypocretin systems secondary to hypothalamic damage may be responsible for decreased hypocretin levels (and some rare hypersomnia cases). Clinical symptoms and other diagnostic findings (such as MRI) are useful in differentiating these cases from narcolepsy, so low hypocretin levels in these diseases do not confound the diagnostic value for narcolepsy.

High percentages of low levels of GBS and ADEM are interesting because they may suggest immune-mediated damage of hypocretin neurons. A similar mechanism may also be involved in hypocretin-deficient idiopathic narcolepsy. Intermediate levels were seen in a neonatal case of PWS prior to the appearance of hypersomnia and obesity. PWS may thus be a model for congenital dysfunction/developmental failure of the hypocretin system. Similarly, the NPC case with cataplectic-like episodes may be a model for acquired deterioration of the hypocretin system by accumulation of lipids in the brain structures responsible for the induction of cataplexy.

There may be some false negatives in the presumed nonnarcoleptic group, as this group did not receive the same series of

evaluations as the narcolepsy group, including polysomnography and MSLT. Nevertheless, with any of the other neurologic disorders, a concomitant diagnosis of narcolepsy is relatively improbable based on their overall clinical presentations. Low CSF hypocretin levels were consistently found in all narcoleptic subjects. In addition, these levels were occasionally found prior to classic narcoleptic signs and symptoms. There may be a true, relatively independent diagnostic utility in measuring CSF hypocretin levels when narcolepsy is suspected in children.

From the Department of Pediatrics (Dr. Arii), Chiba Rosai Hospital, and Division of Neurology (Dr. Tanabe), Chiba Children's Hospital, Departments of Neuropsychiatry (Drs. Kanbayashi, Mishima, Hishikawa, and Shimizu) and Pediatrics (Dr. Sawaishi), Akita University School of Medicine, Department of Pediatrics (Dr. Kimura), Akita Red Cross Hospital, and Department of Pediatrics (Dr. Watanabe), Akita Nakadori General Hospital, Japan; and Center for Narcolepsy (Dr. Nishino), Stanford University, Palo Alto, CA.

Received July 18, 2003. Accepted in final form July 12, 2004.

Address correspondence and reprint requests to Dr. J. Arii, Department of Pediatrics, Chiba Rosai Hospital, 2-16 Tatsumidai-Higashi, Ichihara-shi, Chiba 290-0003, Japan; e-mail: junko-a@muf.biglobe.ne.jp

References

1. Guilleminault C, Pelayo R. Narcolepsy in prepubertal children. Ann Neurol 1998;43:135–142.
2. Palm L, Persson E, Elmqvist D, Blennow G. Sleep and wakefulness in normal preadolescent children. Sleep 1989;12:299–308.
3. Nishino S, Ripley B, Overeem S, Lammers GJ, Mignot E. Hypocretin (orexin) deficiency in human narcolepsy. Lancet 2000;355:39–40.
4. Ripley B, Overeem S, Fujiki N, et al. CSF hypocretin/orexin levels in narcolepsy and other neurological conditions. Neurology 2001;57:2253–2258.
5. Mignot E, Lammers GJ, Ripley B, et al. The role of cerebrospinal fluid hypocretin measurement in the diagnosis of narcolepsy and other hypersomnias. Arch Neurol 2002;59:1553–1562.
6. American Academy of Sleep Medicine. International Classification of Sleep Disorders, rev.: diagnostic and coding manual. Rochester, MN: American Academy of Sleep Medicine, 2001.
7. Kanbayashi T, Yano T, Ishiguro H, et al. Hypocretin-1 (orexin-A) levels in human lumbar CSF in different age groups: infants to elderly persons. Sleep 2002;25:337–339.

Aortic dissection presenting with transient global amnesia-like symptoms

C. Gaul, MD; W. Dietrich, MD; B. Tomandl, PhD; B. Neundörfer, PhD; and F.J. Erbguth, PhD

Diagnostic criteria of transient global amnesia (TGA) are witnessed attacks, clear-cut anterograde amnesia during the attack, absent clouding of consciousness and loss of personal identity, no accompanying focal neurologic symptoms or epileptic features, resolution of attacks within 24 hours, and no recent head injury or active epilepsy.[1] For the etiology of TGA, four main hypotheses have been considered: TIA, epilepsy, migraine, and transient venous ischemia.[1-3] None of these hypotheses fully explains the mechanism of this episodic disease, but the accepted neuroanatomic correlate of TGA is the mediobasal temporal lobe and hippocampus. We present two patients with aortic dissection who provide evidence for an ischemic pathogenesis in TGA.

Case reports. Patient 1. A 47-year-old man was found confused and disoriented. On examination at admission, he asked repetitive questions and was alert but completely disoriented to time and place and only partially oriented to person. The cranial nerve examination showed only a slight anisocoria. The pronator drift test revealed a discrete motor deficit of the left side, accompanied by a mildly increased reflex activity. The cranial CT was unremarkable. The EEG revealed no epileptic discharges. Some hours later, the patient was reoriented with an amnestic gap for the attack's duration, and the neurologic deficit had completely resolved. Because of persistent hypotension, a chest radiograph was taken, which revealed a widening of the mediastinum. A CT scan of the chest and abdomen revealed a dissecting aneurysm (Stanford type A) of the aortic arch starting at the aortic valve, involving both carotid arteries and the left subclavian artery, and continuing into both iliac arteries (figure).

Patient 2. A 61-year-old woman was taken to hospital because of acute chest pain. On admission, she had retrograde amnesia for the past few hours, anterograde amnesia with inability to learn new facts, and repetitious questioning. Neurologic examination revealed a mild right facial paresis. Cranial CT was unremarkable. Five hours after onset of symptoms, she was reoriented with an amnestic gap. Because of the initial thoracal pain and our knowledge of the first reported patient, an aortic dissection was considered. Chest radiograph was normal, but a CT scan of the chest and abdomen revealed a dissection of the aorta (Stanford type A) starting at the aortic valve, involving all supra-aortal branches, and ending above the left renal artery.

Discussion. Patients with TGA can be distinguished into three groups: "pure TGA" patients who fulfill all diagnostic criteria; patients with probable epileptic amnesia; and patients with probable transient ischemic amnesia. The third group includes patients with additional neurologic deficits during the attack as in our patients.[1] Although we found no proof of ischemic lesions in the cranial CT in our patients, the minor neurologic deficits suggested cerebral ischemia. MRI including diffusion-weighted MRI (DWI) would have been helpful to characterize the etiology, but both patients underwent immediate surgery without possibility for further diagnostics. We presume that an aortic dissection can cause a TGA subtype with ischemic etiology, which can be called transient ischemic amnesia. The underlying mechanism may be an embolic vascular occlusion in the posterior circulation, thus causing an embolic TIA with an unusual TGA-like TIA syndrome. The ischemic hypothesis in TGA was enforced by bitemporal hypoperfusion found in brain SPECT.[4] However, patients with TGA have fewer thromboembolic risk factors and smaller risk of cerebral infarction compared with those with TIA.[1] The DWI findings provide conflicting results concerning a possible ischemic mechanism.[5] In one study using DWI in 10 patients with TGA, 7 patients showed an elevated signal intensity in the left or in both temporomesial regions. This was interpreted as a hint of the possible etiologic role of spreading depression.[6] One-third of patients with TGA also have migraine. The low recurrence rate of ~8% in TGA and the different age distribution are arguments against migraine as a pathogenic mechanism.[1] The weakest evidence is

Figure. Multiplanar reconstructions from spiral CT: multiple dissection membranes within the aortic arch are demonstrated with involvement of the supra-aortic branches (arrows).

特集・日常よく見る小児神経疾患に対する薬の使い方

筋疾患

田辺雄三*

Summary

小児筋疾患の内，薬物治療により寛解治癒が望める可能性を持つ自己免疫機序を基盤とした重症筋無力症と皮膚筋炎の薬物治療について概説した．小児重症筋無力症では眼筋型が大部分を占め，抗コリンエステラーゼ剤，副腎皮質ステロイド剤投与により，小児皮膚筋炎は2年程度の副腎皮質ステロイド投与により寛解する可能性が高い．いずれも難治例に対しては，ステロイド・パルス療法，血漿交換，大量ガンマグロブリン療法，免疫抑制剤併用が行われる．

はじめに

薬物療法が行われる小児神経疾患の中では筋疾患は限られたものであるが，いずれも日常臨床上重要な疾患である．ここでは，的確な薬物治療により治癒が期待できる重症筋無力症と皮膚筋炎について，それぞれ疾患の概要，実際の治療薬の使い方，薬剤の副作用を述べる．

〈重症筋無力症〉

疾患の概要

神経筋接合部後シナプス膜のニコチン作動性アセチルコリン受容体に対する自己抗体が産生される事により神経筋伝達障害が生じる．日内変動を伴う筋の易疲労性を特徴とし，臨床的には主に外眼筋を侵す眼筋型，四肢筋あるいは球麻痺症状が主となる全身型に二分される．小児期では眼筋型が多くを占める．

以下によって診断される．(1) テンシロンテスト　塩化エドロフォニウム（アンチレックス）0.2mg/kg 生食10倍希釈30秒程度で静注．外眼筋麻痺改善の程度を観察．(2) 電気生理学的検査　誘発筋電図　反復刺激でM波減衰　(3) 血中抗アセチルコリン受容体抗体 (4) 胸部単純X線，胸部CT，MRIで胸腺腫の有無を確かめる．

薬物治療の実際

小児科領域における重症筋無力症の治療は基本的には成人治療に準じる．すなわち①抗コリンエステラーゼ剤（抗コ剤）②短期免疫療法（血漿交換・ガンマグロブリン大量療法・メチルプレドニゾロンパルス療法）③胸腺摘徐④長期免疫抑制療法（プレドニゾロン・タクロリムス・アザチオプリン・シクロスポリン）である．前述したように小児では眼筋型が多く，抗コ剤，ステロイド治療が中心である．どの方法がもっとも適しているかは治療に対する反応，それぞれの治療法のメリット，デメリットを考慮して決定する．

重症筋無力症における治療プロセスを図1に示した．

①抗コ剤

小児眼筋型治療における第一選択剤である．

薬品名（製品名）	初回投与量(mg)	
	5歳＞	5歳＜
臭化ピリドスチグミン(メスチノン)	5-15	15
塩化アンベノニウム(マイテラーゼ)		

* Yuzo TANABE（部長）：千葉県こども病院第一内科

(0388-7332/04/￥180/論文/JCLS)

	2.5-5	7.5
臭化ネオスチグミン(ワゴスチグミン)		
	5-10	15

いずれも分4が原則．まず半減期の短いメスチノンから試みる．1週間毎に徐々に増量．

症状が改善したとしても，自己免疫病態を変えるわけではない．長期使用により効果が少なくなるが，しばらく休薬期間をおくと再度効果が出現することもある．

副作用：ムスカリン様作用で悪心，嘔吐，腹痛，下痢，発汗を認め，さらにはコリン作動性クリーゼと呼ばれる状態がある．抗コ剤を臨床経過と共に次第に増量していく傾向があり，コリン作動性筋力低下を招くことがある．定期的に減量することにより却って筋力低下が改善するかどうかを確かめるべきである．

②大量ガンマグロブリン療法

血漿交換療法と同じ適応と考えて良い．すなわち，1）胸腺摘徐前あるいは免疫抑制剤効果出現前の筋力低下増悪の軽減，2）難治例，3）筋無力症クリーゼ．効果は1週間以内に出現し，1か月程度持続する．用法，用量は400mg/kg 連日5日間あるいは1g/kg 2日間大量投与．

副作用：頭痛，無菌性髄膜炎，感冒症状

IgA欠損症ではアレルギー反応をおこす可能性がある．当然ながら，ヒト血漿成分由来のものであり未知のリスクを含んでいる点は患者および患者家族へ充分な説明が必要であることは言うまでもない．

③ステロイドホルモン

ステロイドホルモンは細胞性免疫を初めとする様々な免疫抑制作用を有する．投与例の80％程度に有効．プレドニゾロン（プレドニン）1mg/kg朝1回隔日投与から開始し，1－2週ごとに経過をみながら増量，最大量60－80mg/日．増量中に寛解をみれば，その量を最大量として2－3か月用いた後，斬減．減量スケジュールは5mg/週程度ずつ減量開始，最大投与量の半分程度になったら2－3か月かけてゆっくり10mg隔日投与までもっていく．減量中再燃したら，隔日投与で最大量まで増量．その後は初めの2－3倍の時間経過で減量スケジュールを行う．

胸腺摘徐を行う場合も，急激な悪化を防ぐために1mg/kg/日術前に投与．さらに胸腺以外で産生される抗体抑制のため胸腺摘徐後にも投与する．

急速な筋力低下のため初期量を多く設定する場合，少数例ではあるが3週間以内に筋力低下が著しくなる例がある（初期増悪）．このような場合は入院治療を原則とし，血漿交換・大量ガンマグロブリン療法をステロイド内服前に行うことによって初期増悪は回避出来る．ステロイドホルモンの効果は1ヶ月以内に認められる．

副作用：長期間のステロイド療法の副作用は成人に認められるものと基本的に変わりないが，小児で特徴的なことは最低4mg/m²/日程度で成長障害が生じることである．加えて長期ステロイド療法は成人期以降の骨粗鬆症に影響を与えるとされる．骨密度に影響を与える総ステロイド量は平均17g程度．これは9年間10mg隔日投与に相当．いずれにせよ，重症筋無力症小児は成人期以降も長期間のステロイド療法を必要とすることもあり，投与方法，免疫抑制剤併用，大量ガンマグロブリン療法，胸腺摘徐なども視野に入れてステロイド療法を考慮すべきである．

重症例あるいはステロイドホルモン内服療法で効果を示さない場合，メチルプレドニゾロン（ソル・メドロール）30mg/kg（5%ブドウ糖200ml溶解，2時間点滴静注）連日3日間を1クールとし投与する方法も効果的である．ステロイドパルス療法後はプレドニゾロン内服隔日投与を行う．

④免疫抑制剤

ステロイド抵抗性・依存性，あるいは副作用が強くステロイド剤の減量を必要とする場合などには免疫抑制剤を併用する．

アザチオプリン（イムラン）はステロイド用量低減効果を示し，ステロイド剤単独使用に比べ予後良好な結果が出ている．用量は1－2.5mg/kg/日で開始，各週0.5mg/kg/日ずつ増量していく．治療効果の発現には数か月以上かかる．副作用としては感冒様症状，肝機能異常，白血球減少，汎血球減少，催奇形性などがある．

シクロフォスファマイド（エンドキサン）はアザチオプリンより有効率が高く迅速な効果を呈す一方，不妊，催奇形性，発ガン性などの副作用が強いとされる．用量は1－2mg/kg/日内服．

タクロリムス　（プログラフ）0.05mg/kg/日1日1回夕食後服用．成人例で有効性が確認され，最近，小児難治例でも使用され始めている．

副作用として移植時のように大量に使用する場合，腎障害，脳症などが報告されているが低用量の使用では副作用は少ない．

シクロスポリン（サンディミュン）

筋力低下改善，抗AchR抗体低下，ステロイド用量低減効果が認められている．2か月以内に効果出現．5mg/kg/日分二内服，副作用は腎毒性，高血圧，頭痛など．

⑤クリーゼの治療

急激な筋力低下により嚥下障害，呼吸困難の症状が出現したときクリーゼと呼ぶが，原疾患の急激な進行による筋無力症性クリーゼと抗コ剤の過量投与によるコリン作動性クリーゼがある．いずれのクリーゼも起こる可能性があることを念頭に置くべきであるが，実際に呼吸困難が生じたときは，まず気道確保を行い人工呼吸器下に置き，輸液を行い全身状態の改善，抗生剤投与などの感染症治療を行う．抗コ剤はすぐに中止する．両方のクリーゼの鑑別は必ずしも容易ではないが，テンシロンテストを行い症状が改善するようであれば，筋無力症性クリーゼと考えネオスチグミン（ワゴスチグミン）0.25－0.5mg皮下注または筋注/毎4時間をおこない速やかに経口剤に切り替える．さらには短期効果目的で血漿交換，大量ガンマグロブリン療法も考慮する．寛解目的でステロイド剤も開始する．

図1に小児重症筋無力症における治療方針を示し，表1に重症筋無力症を悪化させる薬剤をリストアップした．

〈皮膚筋炎〉

疾患の概要

遺伝的要因に加えウイルス感染などを契機に免疫異常がおこり，全身の血管炎により特徴的な皮膚病変と筋内血管炎による筋線維壊死，再生を生じる疾患である．小児では皮下の石灰化を伴うこと，悪性腫瘍の合併はないこと，予後良好例があることなどのため若年性（小児）皮膚筋炎と呼ばれ成人例とは区別されている．

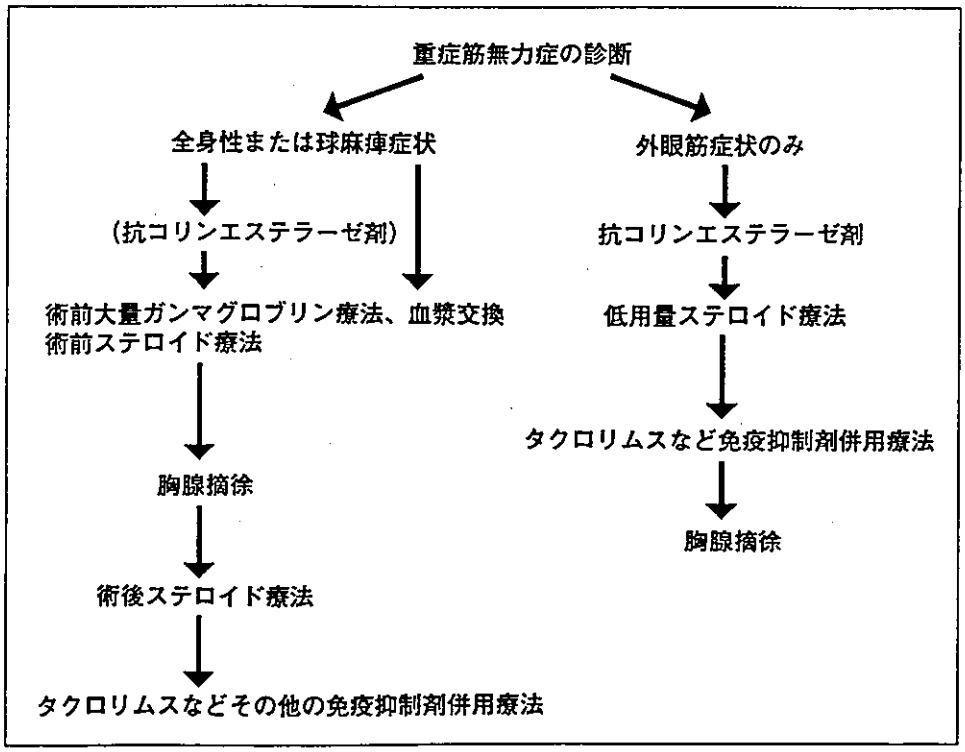

図1　小児重症筋無力症における治療方針

表1 重症筋無力症を悪化させる薬剤

①D-ペニシラミン
②サクシニルコリン，d-ツボクラリン，ベクロニウム，神経筋ブロック剤
③キニーネ，キニジン，プロカインアミド
④トブラマイシン，ゲンタマイシン，カナマイシン，ネオマイシン，ストレプトマイシン，コリスチン，エリスロマイシン，シプロフロキサシン，フルオロキノロン
⑤βブロッカー（プロプラノロール，マレイン酸チモロール点眼液）
⑥カルシウムチャンネルブロッカー
⑦ヨード造影剤
⑧マーロックスなどのマグネシウム製剤
⑨利尿薬（カリウム喪失作用を持つもの）

急性発症の場合には近位筋優位の筋力低下に加え，発熱，筋痛，レイノー現象を認める．

慢性経過例では，筋力低下のみのこともあり筋ジストロフィーとの鑑別が困難なことがある．

診断

診断は以下の所見を認めれば困難ではない．①上眼瞼のヘリオトロープ疹などの皮膚炎症状，近位筋優位の筋力低下などの筋炎症状②血清クレアチンキナーゼなどの筋原性酵素の上昇（急性期には参考になる）③神経原性あるいは筋原性筋電図所見④血管周囲炎症細胞浸潤，筋束周囲萎縮を中心とした筋病理所見．

治療

小児例は特にステロイド剤に対する反応が良好で早期診断，早期治療開始が重要である．

プレドニゾロン2mg/kg/日（最高100mg/日）早朝分1を連日1か月程度投与し症状の改善を見たら，5mg/月漸減し半量すなわち1mg/kg/日程度から2.5mg/月のペースで慎重に減量していく．この際血清クレアチンキナーゼ，アルドラーゼ値の減少が即筋力低下の改善を意味するわけではない．したがって，筋原性酵素を指標に治療プランを考慮することは適切ではない．あくまでも，筋力低下，日常生活動作の改善度を中心に考えるべきである．ステロイド治療に対する反応の良い例では，投与開始後2週間程度で筋力低下の改善，血清クレアチンキナーゼの低下が見られる．再燃をおこさない最低量を維持量とするが，維持量は0.5mg/kg/日前後となることが多い．投与中止まで2年以上かかる．消化管の血管炎による潰瘍，穿孔を来たす例あるいは拘束性呼吸障害を合併し急激な経過をとる例ではステロイドパルス療法が行われる．再燃のため最終的に減量中止が望めないステロイド依存例．副作用が強く出る場合．最初の1－2か月投与で臨床的な改善が認められない例，筋力低下，呼吸不全が急速に進行する例では免疫抑制剤の併用を考慮する．免疫グロブリン大量療法も行われる．免疫抑制剤，免疫グロブリン大量療法は前記の重症筋無力症の治療方法に準じる．

プレドニゾロン長期使用では一般的な副作用に加え，ステロイドミオパチーの鑑別を必要とすることがある．投与後3ヶ月以降に症状があらわれやすく，投与量，投与期間とは必ずしも一致しない．原疾患に比べ血清CK値上昇少なく，筋電図上筋原性変化が乏しく，病理的にはタイプ2線維萎縮を中心とした筋原性変化が認められる．ステロイドを減量または中止で筋力は回復する．

文 献

1) Andrews PI, Sanders DB : Juvenile Myasthenia Gravis. In Jones HRJr, DeVivo DC, Darras BT (eds) : Neuromuscular Disorders of Infancy, Childhood, and Adolescence: A Clinician's Aproach. Philadelphia, Butterworth Heinemann, 2003, pp585
2) 加我牧子，佐々木征行，須貝研司編著：精神神経センター小児神経科診断・治療マニュアル，診断と治療社，2003.
3) Engel AG eds : Myasthenia Gravis and Myasthenic Disorders. New York, Oxford University Press, 1999.
4) Fenichel GM : Clinical Pediatric Neurology. Philadelphia, W. B. Saunders, 2001.

* * *

ANTIOXIDANTS & REDOX SIGNALING
Volume 6, Number 3, 2004

Forum Original Research Communication

Mitochondrial Signal Lacking Manganese Superoxide Dismutase Failed to Prevent Cell Death by Reoxygenation Following Hypoxia in a Human Pancreatic Cancer Cell Line, KP4

FUTOSHI HIRAI,[1,2] SHIGEATSU MOTOORI,[1] SHIZUKO KAKINUMA,[2] KAZUO TOMITA,[2,3] HIROKO P. INDO,[3] HIROTOSHI KATO,[2] TAKETO YAMAGUCHI,[1] HSIU-CHUAN YEN,[4] DARET K. ST. CLAIR,[5] TETSUO NAGANO,[6] TOSHIHIKO OZAWA,[2] HIROMITSU SAISHO,[1] and HIDEYUKI J. MAJIMA,[2,3,7]

ABSTRACT

One of the major characteristics of tumor is the presence of a hypoxic cell population, which is caused by abnormal distribution of blood vessels. Manganese superoxide dismutase (MnSOD) is a nuclear-encoded mitochondrial enzyme, which scavenges superoxide generated from the electron-transport chain in mitochondria. We examined whether MnSOD protects against hypoxia/reoxygenation (H/R)-induced oxidative stress using a human pancreas carcinoma-originated cell line, KP4. We also examined whether MnSOD is necessarily present in mitochondria to have a function. Normal human MnSOD and MnSOD without a mitochondrial targeting signal were transfected to KP4 cells, and reactive oxygen species, nitric oxide, lipid peroxidation, and apoptosis were examined as a function of time in air following 1 day of hypoxia as a H/R model. Our results showed H/R caused no increase in nitric oxide, but resulted in increases in reactive oxygen species, 4-hydroxy-2-nonenal protein adducts, and apoptosis. Authentic MnSOD protected against these processes and cell death, but MnSOD lacking a mitochondrial targeting signal could not. These results suggest that only when MnSOD is located in mitochondria is it efficient in protecting against cellular injuries by H/R, and they also indicate that mitochondria are primary sites of H/R-induced cellular oxidative injuries. *Antioxid. Redox Signal.* 6, 523–535.

INTRODUCTION

It has been known that hypoxic cells exist in tumors (7, 39) because of irregular localization of blood vessels. The hypoxic cells are resistant to various anticancer treatment modalities, such as radiation, bleomycin, *cis*-platinum, major chemotherapeutic agents utilized in the treatment of cancer, etc. (for review, see 16), which are all major treatments in cancer therapy. These treatment modalities are known to generate reactive oxygen species (ROS) (4, 30, 49). These modalities are effective in killing tumor cells; one of the mechanisms of tumor killing could be related to ROS

[1]First Department of Medicine, Chiba University, School of Medicine, Chiba 260–0856, Japan.
[2]National Institute of Radiological Sciences, Chiba 260-8555, Japan.
[3]Department of Oncology, Kagoshima University Graduate School of Medical and Dental Sciences, Kagoshima 890-8544, Japan.
[4]School of Medical Technology, Chang Gung University, Kwei-Shan, Tao-Yuan 333, Taiwan.
[5]Graduate Center for Toxicology, University of Kentucky, Lexington, KY 40536, U.S.A.
[6]Graduate School of Pharmaceutical Sciences, The University of Tokyo, Tokyo 113-0033, Japan.
[7]Department of Space Environmental Medicine, Kagoshima University Graduate School of Medical and Dental Sciences, Kagoshima 890-8544, Japan.

generation. Further, hypoxic cells may be related to the development of metastasis (31). Hypoxic cells often become reoxygenated after a dose of radiation or intermittent opening of blood vessels (6, 42). This phenomenon has been called reoxygenation (42).

Ischemia/reperfusion (I/R) in a normal brain causes oxidative damage to neuronal cells (for review, see 20, 25). Pathologic events caused by transient tissue hypoxia followed by oxygen reperfusion occur in numerous other tissues (for review, see 10). The pathologic changes encountered following reperfusion of an ischemic organ include an immediate generation of ROS, as well as subsequent inflammatory responses, which lead to a second stage of further ROS generation at the sites of damage. ROS generation following I/R has been examined in various experimental systems *in vivo* and *in vitro* (20). The injuries caused by I/R also occur in organ transplantation (10). One method to increase the effectiveness of organ transplantation may depend on methods to prevent oxidative stress. Clinical trials have been performed to determine whether antioxidant substances will prevent hypoxic-induced injury (10, 20). The use of gene therapy to reduce redox-mediated damage following such I/R injuries is also a subject for clinical consideration (10).

Many neuronal diseases, such as Alzheimer's disease, Parkinson's disease, and amyotrophic lateral sclerosis, and other diseases, such as aging, diabetes, premature babies, and cancer, are now believed to result from oxidative stress (12, 24, 43). Involvement of oxidative stress in tumor tissue is a subject of potentially great importance. Reoxygenation following hypoxia in tumor tissue has been implied to result in better prognosis after radiation therapy, although this hypoxia might also cause acceleration of tumor growth. However, how hypoxia/reoxygenation (H/R) affects tumor cell viability, and the subcellular mechanism(s) involved, have not been well elucidated. Possible changes in tumors may result from mitochondrial degeneration, as well as from subsequent ROS generation in cells (10). Several studies have shown that mitochondria produce superoxide, mainly from complex I and III of the electron transport system, which is located in the inner membrane of mitochondria (5, 36). Production of ROS from the electron transport chain may result in oxidative stress in cells, and may result in apoptotic cell death (23–25, 43). Manganese superoxide dismutase (MnSOD) is an essential enzyme, which scavenges superoxide located in mitochondria (44). The biological importance of MnSOD is demonstrated by the following: (a) A lack of the MnSOD gene in *Escherichia coli* and yeast makes them hypersensitive to oxidative stress (8, 11, 41). (b) Homozygous mutant mice lacking MnSOD died within the first 10 days after birth and showed dilated cardiomyopathy, an accumulation of lipid in the liver and skeletal muscle, and metabolic acidosis (21). (3) Mutant mice lacking MnSOD showed degenerative injury of large central nervous system neurons, particularly in the basal ganglia and brainstem, associated with damaged mitochondria. Also, these mice showed progressive motor disturbances characterized by limb weakness, rapid fatigue, and circling behavior (18). (d) Transfection of MnSOD cDNA into cultured cells rendered the cells resistant to paraquat- (32), tumor necrosis factor- (13, 47), doxorubicin- (13), mitomycin C- (13), radiation- (13, 27, 35), alkaline- (23), and chemical-induced hypoxia (15), cigarette smoke-induced cytotoxicity (34), and radiation-induced neoplastic transformation (33). (e) The expression of human MnSOD genes in transgenic mice protected the mice against oxygen-induced pulmonary injury (45) and adriamycin-induced cardiac toxicity (48). Thus, the expression of MnSOD is essential for the survival of aerobic life and the development of cellular resistance to oxygen radical-mediated toxicity.

MnSOD has a leader sequence to target mitochondria [mitochondrial targeting signal (MTS)]. This targeting signal translates to an oligopeptide consisting of 24 amino acids (14). The gene is transcribed in the nucleus, translated in the cytosol, and transported into mitochondria, where the precursor is cleaved and the protein undergoes maturation (22, 26). The localization of MnSOD in mitochondria is dependent on the presence of the signal. However, whether the enzyme could have an antioxidative function when it is present in the cytosol remains unclear.

In these studies, we examine the role of mitochondria-localized MnSOD in prevention against H/R-induced oxidative injuries, using a human pancreatic tumor-derived cell line, KP4, following H/R treatment. To elucidate further the significance of mitochondrial localization, MnSOD without the MTS gene was also tested using transfection in the same cell system.

MATERIALS AND METHODS

Cell lines

A pancreatic cancer cell line, KP4 (28), was purchased from the Riken Cell Bank (Tsukuba, Japan). pCR3.1-Uni plasmid (Invitrogen, Carlsbad, CA, U.S.A.) containing a sense human MnSOD cDNA insert was a kind gift of Dr. Akashi (National Institute of Radiological Sciences, Chiba, Japan) (27). A sequence analysis of the MnSOD gene in the construct showed that the sequence was identical to the accession number Y00472, except that C (nucleotide 113) was changed to T, and C (nucleotide 529) was changed to G, which changed alanine to valine and glutamine to glutamic acid, respectively (27). The KP4 cell was transfected using the GenePORTER transfection procedure (Gene Therapy Systems, San Diego, CA, U.S.A.) according to the manufacturer's instructions. In brief, cells were plated for 24 h before transfection at 60% confluence in a 60-mm dish. The cells were stably transfected with 5 μg of pCR3.1-Uni plasmids containing a sense human MnSOD cDNA insert, and linearized by Sca I, in a serum-free Dulbecco's modified Eagle medium (DMEM) (Life Technologies, Inc., Grand Island, NY, U.S.A.). The cells were also transfected with the same human MnSOD construct, but without an MTS [mito(−) MnSOD], which encodes 24 amino acids. The controls were transfected with pCR3.1-Uni plasmids without a human MnSOD cDNA insert and linearized by Sca I. Stable clones of both MnSOD and control plasmid transfectants were selected with Geneticin (Life Technologies, Inc.) at a final concentration of 500 μg/ml. Selected cellular clones that expressed MnSOD (MnSOD-5, -9, and -10), MnSOD without a targeting precursor [mito(−)-4, -6], selectable marker alone (vec-1 and -2),

and the parental cell (KP4) were used in all of the experiments. Selected clones were routinely maintained in DMEM containing 10% fetal bovine serum (JRH Biosciences, Lenexa, KS, U.S.A.) and 500 μg/ml Geneticin at 37°C in humidified air containing 5% CO_2.

To identify the localization of MnSOD and mito(−) MnSOD, KP4 cells were also transfected with pEGFP expression plasmid with the *MnSOD* gene or the *MnSOD* gene lacking MTS, which encodes the entire open reading frame of MnSOD or the MnSOD lacking a mitochondria targeting peptide, and also the mitochondria targeting peptide alone. To construct pEGFP expression plasmids, the cDNAs were incised with *Eco* RI and *Hind* III from the PCR products and inserted into the pEGFP-N1 expression vector (Clontech, San Diego, CA, U.S.A.). The construct was transformed into an XL1 Blue competent cell (Stratagene, La Jolla, CA, U.S.A.) and purified with a QIAFilter Plasmid Kit (QIAGEN, Valencia, CA, U.S.A.). The product was then transfected into cells using the GenePORTER 2 (Gene Therapy Systems), using the same method as described in the pCR3.1-Uni plasmid transfection procedure above. The transfected cells were visualized using a CSU-10 confocal laser scanning unit (Yokogawa Electric Co., Tokyo, Japan) coupled to an IX90 inverted microscope with a UPlanAPO X40 objective lens (Olympus Optical Co., Tokyo, Japan), and a C5810-01 color chilled 3CCD camera (Hamamatsu Photonics K. K., Hamamatsu, Japan). The cells were excited at 488 nm, and the emission was filtered using a 515-nm barrier filter. To ascertain localization of mitochondria, the cells were stained with MitoTracker Red CMXRos (Molecular Probes, Eugene, OR, U.S.A.), then visualized using a confocal laser scanning microscope excited at 488 nm, whereas the emission was filtered using a 580-nm barrier filter. A merged double image of (GFP) and MitoTracker was taken using a confocal laser scanning microscope excited at 488 nm, and the emission was filtered using a double-window barrier filter, of which the ranges were 510–590 and 580–620 nm.

In vitro *biological experimental system for hypoxia and PO_2 measurement system*

Biological experiments were performed in a hypoxic chamber [Anaerobic System MIP-1025 (Forma Scientific, Marietta, OH, U.S.A.)], which was specially modified to culture mammalian cells. The conditions inside the chamber were maintained with 95% humidified nitrogen plus 5% CO_2. The medium PO_2 in a representative flask was measured with MT 5000S (MTGiken, Tokyo, Japan), which was designed and made especially for our experimental system. This equipment included a small electrode (0.2 mm in diameter), which could detect PO_2 at a level as low as 0.1 mm Hg. A hypoxic condition of <8 mm Hg was maintained throughout the experiments. For H/R treatment, cells were maintained in hypoxia for 24 h followed by subsequent exposure to air.

Superoxide dismutase (SOD) activity gel assay

A nondenatured gel assay for SOD activity was performed according to a previously described method (3) with slight modifications. Cells were sonicated in a 50 m*M* potassium phosphate buffer (pH 7.8). Fifty micrograms of protein per lane was electrophoresed through a nondissociating riboflavin gel consisting of 5% stacking gel (pH 6.8) and 12% running gel (pH 8.8) at 4°C. To visualize SOD activity, gels were first incubated in 2.43 m*M* nitro blue tetrazolium (Wako Pure Chemical Industries, Ltd., Osaka, Japan) in deionized water for 20 min, and then in 0.028 m*M* riboflavin (Wako Pure Chemical Industries, Ltd.) and 280 m*M* TEMED (*N,N,N′,N′*-tetramethyl ethylenediamine; Sigma Chemical Co., St. Louis, MO, U.S.A.) in a 50 m*M* potassium phosphate buffer (pH 7.8) for 15 min in the dark. Gels were then washed in deionized water and illuminated under a fluorescent light until clear zones of SOD activity were evident. The images were obtained as TIFF files by a CCD camera in connection with a Power Macintosh G4 (Apple Computer, Inc., Cupertino, CA, U.S.A.). The bands of MnSOD were quantified by NIH Image 1.61, which is available on the Internet via a file-transfer protocol from http://rsb.info.nih.gov/nih-image/download.html. The MnSOD activity of the parental cell was used as the reference, and the relative MnSOD activities of other cells were normalized to those in the parental cells. The mean of the integrated density obtained from three independent experiments was used as a representative value for the experiment.

RT-PCR detection in MnSOD cells and mito(−) cells

Total RNA was isolated from cultured cells using the acid guanidinium–phenol–chloroform method (9). First-strand cDNA was synthesized using Moloney leukemia virus reverse transcriptase (TOYOBO, Tokyo, Japan) with an antisense primer, MnGPB 5′ CCCGAATTCCCTTTTTGCAAGCCATGTATCT 3′. A subsequent PCR was then performed using the same antisense primer, MnGPB, and a sense primer, MnGPA 5′ GGGAAGCTTTGGCTTCGGCAGCGGCTTCAG 3′, which is for detecting a whole range of normal MnSOD mRNA, or a sense primer, Mnmt-GPA 5′ GGGAAGCTTATGAAGCACAGCCTCCCCGACCTG 3′, which is for detecting MnSOD lacking MTS mRNA, using ExTaq DNA polymerase (TaKaRa, Tokyo, Japan) (Fig. 1). PCR was conducted in a PerkinElmer Cetus Thermal Cycler for 31 cycles. After 5 min at 94°C and 5 min at 60°C, amplification was performed for a cycling profile consisting of extension at 72°C for 1 min, denaturation at 94°C for 30 s, and annealing at 60°C for 30 s, followed by final extension at 72°C for 10 min. The PCR products were analyzed electrophoretically in a 1.5% agarose gel with ethidium bromide staining. An image was obtained, and the bands were quantified with an image quantifier (440CF; Kodak, New Haven, CT, U.S.A.)

Microscopic assessment of nuclear chromatin condensation and fragmentation

Cells grown on glass-bottom (35 mm) dishes (MatTek Corp., Ashland, MA, U.S.A.) were stained with a fluorescent dye, Hoechst 33342 (Molecular Probes). At 0, 0.25, 0.5, 1, 3, and 5 h after 1 day of hypoxia, the cells were fixed for 30 min in a solution containing 4% formaldehyde in phosphate-buffered saline (PBS), and then incubated in PBS with 1 μg/ml of the dye for 30 min. The cells were washed twice

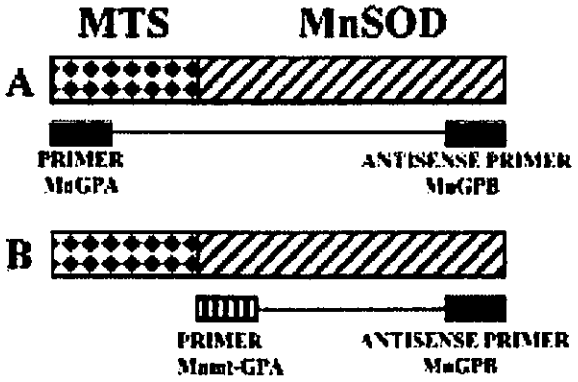

FIG. 1. Schematic diagram of MnSOD gene and primer setting. (A) Construct and primer range for MnSOD and primers used to generate and detect full-length MnSOD cDNA and mRNA. (B) Construct of the full-length MnSOD and primers used to generate and detect MTS-lacking MnSOD cDNA and mRNA.

with PBS and then twice with water. Fluorescence was visualized using an IX90 inverted microscope with a UPlanAPO 20× objective lens (Olympus Optical Co.). The dye was excited at 340 nm, and the emission was filtered with a 510-nm barrier filter. Photographs of microscope fields were taken using a C5810–01 color chilled 3CCD camera (Hamamatsu Photonics K.K.). More than 500 cells per culture dish were counted, and counts were made in three separate cultures per each H/R treatment. Analyses were performed without any knowledge of the H/R treatment history of the culture dishes. The percentage of apoptotic cells (apoptotic index) in each culture dish was determined.

Bioimaging of nitric oxide (NO)

Diaminofluoresceins (DAFs) (Daiichi Pure Chemicals, Tokyo, Japan) are fluorescent indicators for NO (17). They do not react with NO itself, but with NO+ equivalents, such as nitric trioxide (N_2O_3), which are produced by autoxidation of NO. Diaminofluorescein-FM diacetate (DAF-FM DA), which was a kind gift from Daiichi Pure Chemicals, is a newly synthesized DAF, which permeates well into cells and is quickly converted into water-soluble DAF-FM by esterases in the cytosol, where the dye can remain for a long time. Under aerobic conditions, DAF-FM traps NO to yield highly fluorescent triazofluoresceins (DAF-FM Ts) by nitrosation and dehydration. DAF-FM Ts are not formed in the presence of NO. Glass-bottom (35 mm) dishes (MatTek Corp.) with monolayers were prepared for staining with DAF-FM DA. At 0, 1, 2, 3, and 6 h after a H/R treatment, the cell culture medium was replaced with a modified Hanks' balanced salt solution containing 10.0 m*M* HEPES, 1.0 m*M* $MgCl_2$, 2 m*M* $CaCl_2$, and 2.7 m*M* glucose adjusted to pH 7.3 ± 0.05. The cells were then loaded with 10 μ*M* DAF-FM DA by incubation for 30 min at 37°C. Bioimages of DAF-FM DA were acquired using a CSU-10 confocal laser scanning unit (Yokogawa Electric Co.) coupled to an IX90 inverted microscope with UPlanAPO X20 objective lens (Olympus Optical Co.) and C5810–01 color chilled 3CCD camera (Hamamatsu Photonics. K.K.). The DAF-FM DA was excited at 488 nm, and the emission was filtered using a 515-nm barrier filter. The intensity of the laser beam, the exposure time of the 3CCD camera, and the gain of the amplifier were held at 500 μW, 1.0 s, and 18 db, respectively, to allow quantitative comparisons of the relative fluorescent intensity of the cells between groups. Cells were chosen and scanned at more than three spots for analysis on a random basis. The values for the average fluorescence intensity per cell were obtained using IPLab Spectrum version 3.0 (Scanalystics Inc., Fairfax, VA, U.S.A.) software with some modification of the program by the author (H.J.M). The fluorescent intensity (which was acquired by confocal laser microscopy and analyzed by computer) following H/R treatment divided by the intensity of no-treatment intact cells was calculated as the relative fluorescent intensity, which indicates the "increment" of the intensity induced by H/R treatment in each cell. Note that the relative fluorescent intensity is *not* the ratio of the fluorescent intensity to the control plasmid transfected cells or parental cells.

Relative levels of mitochondrial ROS

Dihydrorhodamine 123 (dhRho) (Molecular Probes) is an oxidation-sensitive lipophilic dye that enters a cell and fluoresces when oxidized by mitochondrial ROS to the positively charged rhodamine 123 derivatives. The relative level of mitochondrial ROS loaded with dhRho was quantified by a confocal laser microscope image using the same procedures described for DAF measurements, except that the final concentration of the dye used in the study was 10 μg/ml.

Immunofluorescent staining for 4-hydroxy-2-nonenal (HNE)

Glass-bottom (35 mm) dishes (MatTek Corp.) with monolayers were prepared for immunofluorescent staining with a monoclonal antibody directed against proteins modified by the major membrane lipid peroxidation product, HNE. This monoclonal antibody (NOF Corp., Tokyo, Japan), specific for HNE-modified proteins, was raised by immunizing mice with an HNE-modified keyhole limpet hemocyanin conjugate (40). The antibody was tested for cross-reactivity toward glutaraldehyde, formaldehyde, 1-hexanal, 2-hexanal, 4-hydroxy-2-hexanal, and 2-nonenal. Enzyme-linked immunosorbent assays with these potential competitors were performed. The results indicated that the anti-HNE antibody is highly specific to HNE-derived modifications to protein. At 0, 1, 2, 3, and 6 h after the H/R treatment, cells were fixed with 4% formaldehyde/PBS at room temperature for 30 min and then rinsed twice with PBS, and membranes were permeabilized by incubation in 95% ethanol with 5% acetic acid for 10 min. After washing with PBS twice, the cells were incubated for 4 min in a blocking solution(1% bovine serum albumin in PBS) and for 1 h in anti-HNE mouse monoclonal antibody at a dilution factor of 1:200. The cells were rinsed twice with 0.1% bovine serum albumin in PBS and reincubated with Alexa Fluor 488 goat anti-mouse IgG (H+L) conjugate (Molecular Probes) for 1 h at room temperature. Image acquisition and analysis were similar to that of DAF-FM DA, except that the exposure time of the 3CCD camera was 10 s.

Statistical analysis

A statistical analysis was performed by an analysis of variance, followed by Fisher's post hoc tests. A p value of <0.05 was considered to be statistically significant. Data were presented as the means ± SE. Calculations were performed with a statistical package, StatView 5.0J (SAS Institute Inc., Cary, NC, U.S.A.), on a Power Macintosh G3 (Apple Computer, Inc.).

RESULTS

Isolation of KP4 transfectants expressing MnSOD and mito(−) MnSOD

The production of active MnSOD in these transfectants was investigated in cell lysates. The parent KP4 cells, two vector clone transfectants (vec-1 and -2) (from six clones), two mito(−) MnSOD clones [mito(−)-4 and -6] (from six clones), and three MnSOD clones (MnSOD-5, -9 and -10) (from 12 clones) were examined for MnSOD activity. The intensity of MnSOD was semiquantified from the captured image. MnSOD activity of the parental cells was normalized to 1, and the relative MnSOD activities of the other cells were calculated (Table 1). The increase in MnSOD activity in the clones MnSOD-5, -9, and -10 was clearly detectable, *i.e.*, the MnSOD activity in the MnSOD-transfected cells was greater than that in the control cells. The relative activities of MTS-lacking MnSOD [mito(−)] transfectants were also greater compared with that in the control cells, although they were generally slightly less than those in the MnSOD clones.

RT-PCR detection of mRNA in MnSOD cells and mito(−) cells

To ascertain the expression of MnSOD and MnSOD lacking MTS, total cellular RNA was first reverse-transcribed into cDNA with an antisense primer, MnGPB, and then subsequently amplified by PCR. To examine the full-range MnSOD including MTS gene expressions, a sense primer (MnGPA) and an antisense primer (MnGPB) were used for PCR amplification, whereas to examine the MnSOD without MTS gene expression, a sense primer (Mnmt-GPA) and an antisense primer (MnGPB) were used for PCR amplification (Fig. 1). Increased MnSOD mRNA levels were confirmed in MnSOD-5, -9, and -10 using the MnGPA primer (Fig. 2A). However,

TABLE 1. RELATIVE INTENSITY OF MNSOD ACTIVITY

Cell line	*Relative intensity*
KP4	1
Vec-1	1.091 ± 0.040
Vec-2	1.207 ± 0.292
Mito(−)-4	2.320 ± 0.494
Mito(−)-6	1.861 ± 0.191
MnSOD-5	2.471 ± 0.362
MnSOD-9	3.024 ± 0.482
MnSOD-10	2.570 ± 0.505

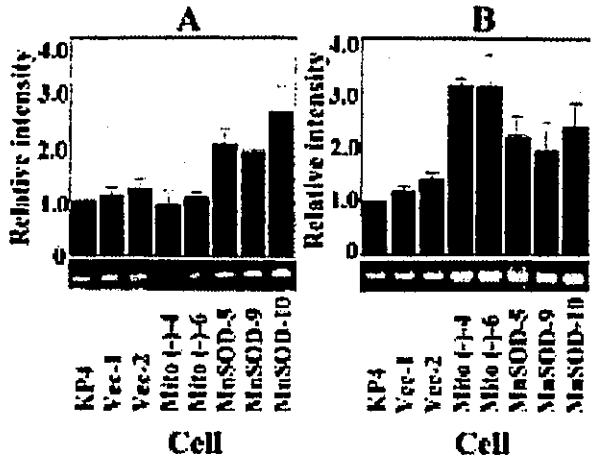

FIG. 2. RT-PCR detecting mRNA of the full length of normal MnSOD, or MTS-lacking MnSOD. (A) The full-length MnSOD including MTS gene expression, a sense primer (MnGPA), and an antisense primer (MnGPB) were used for PCR amplification. The full-length mRNA levels were higher in MnSOD-5, -9, -10 compared with that in the controls and mito(−) clones. **(B)** MnSOD without MTS, a sense primer (Mnmt-GPA), and an antisense primer (MnGPB) were used for the PCR amplification. The transfected mRNA was higher in MnSOD-5, -9, -10, mito(−) -4 and -6 transfectants, compared with the untransfected and vector alone controls.

when the Mnmt-GPA primer was used, not only did the mRNA for MnSOD-5, -9, and -10 increase, but higher mRNA levels of the MnSOD products for mito(−)-4 and -6 transfectants were observed (Fig. 2B). These results are consistent with those found for MnSOD activity and demonstrate that the transfection of MnSOD lacking MTS vectors was successful in mito(−) -4 and -6 transfectants.

Effect of MnSOD on H/R-induced apoptotic cell death

To determine the effect of H/R treatment on apoptotic cell death, we performed a microscopic assessment of nuclear chromatin condensation and fragmentation assay using Hoechst 33342 staining. For control experiments, we examined the change in the apoptotic index (number of apoptotic cells/500 cells counted) in air (Fig. 3A) or hypoxic conditions alone (Fig. 3B). As shown in Fig. 3, in cells grown up to 5 days in either air or hypoxic conditions, no increase in the apoptotic index was observed. In H/R experiments (Fig. 4), the apoptotic index was determined in cells cultured in air for 0, 0.25, 0.5, 1, 3, and 5 days after the 1-day hypoxia treatment. Except for MnSOD-5, -9, and -10, the apoptotic index significantly increased at 1 day, and by 5 days declined to the control levels in all cells. The absolute number of apoptotic cells and the relative index, which was calculated as the ratio of apoptotic cell count on day 1 to that on day 0, are listed in Table 2. The results show that the relative apoptotic index was suppressed in the full-length MnSOD transfected cells compared with that of the KP4, vec-1 and -2, and mito(−) transfectants. This result indicates that only when MnSOD is

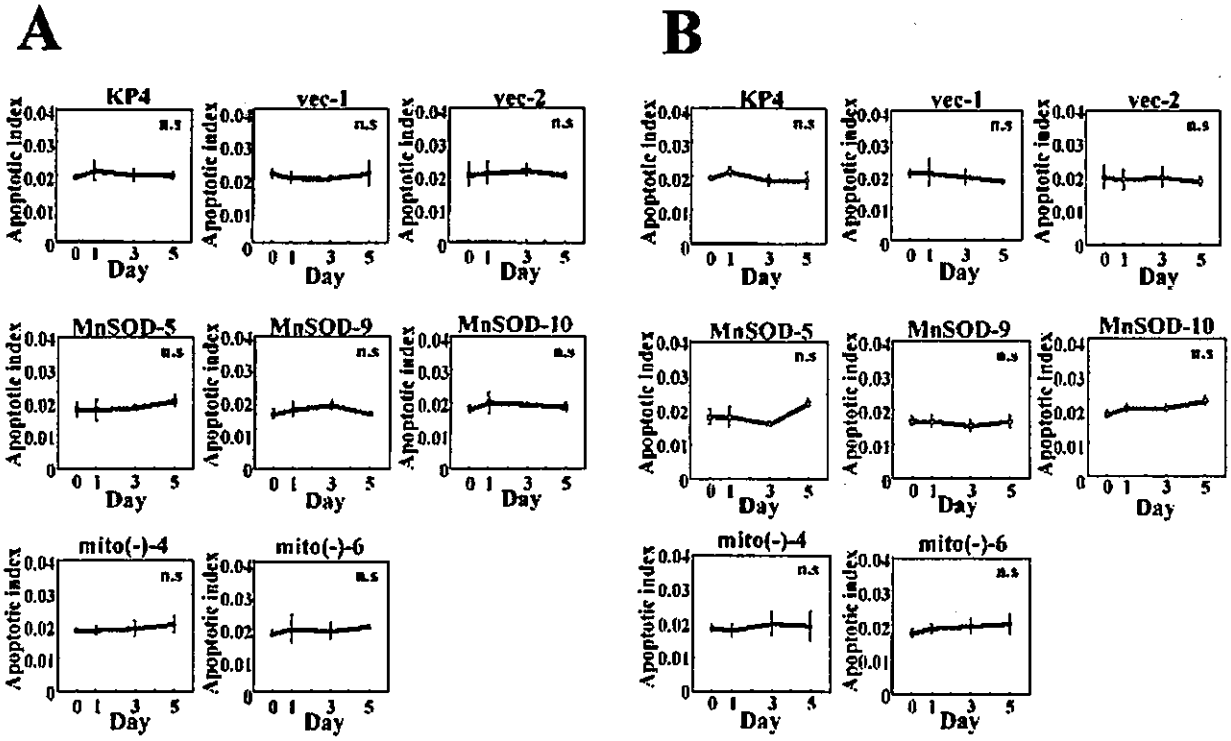

FIG. 3. No change in the apoptotic index as a function of time in air or hypoxic conditions. The change in apoptotic index (number of apoptotic cells/500 cells counted) in air (**A**) or hypoxia alone (**B**) is presented. n.s, not significant.

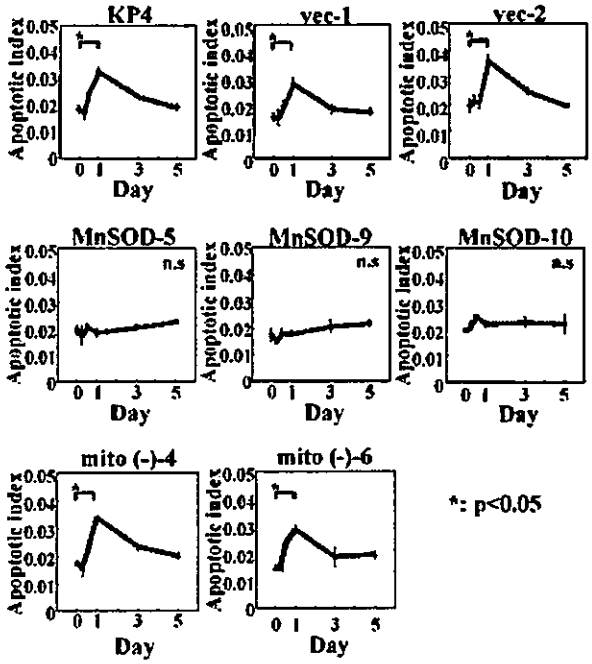

FIG. 4. Apoptotic index for H/R condition. The apoptotic index in each cell line at 0, 0.25, 0.5, 1, 3, and 5 days in air after 1 day of hypoxia treatment (H/R treatment) was determined. With the exception of MnSOD-5, -9, and -10, the apoptotic index increased to a maximum in 1 day, followed by a decline in all cells. The full-length MnSOD, and not MTS-lacking MnSOD, suppresses H/R treatment-induced apoptosis. n.s, not significant; $^{*}p < 0.05$.

localized in the mitochondria can it suppress H/R-induced apoptosis.

MnSOD does not influence hypoxia-induced NO generation

To determine the effect of MnSOD on H/R treatment-induced intracellular NO generation, a dye sensitive to a change in the intracellular NO, DAF-FM DA, was used. To ascertain NO generation ability in every cell type, we irradiated cells with 15 Gy and examined NO generation at 2 h fol-

TABLE 2. NUMBER OF APOPTOTIC CELLS AND THE RELATIVE APOPTOTIC INDEX

Cell line	*Apoptotic cell day 1/day 0**	*Relative apoptotic index*
KP4	16.33 ± 0.88 / 9.33 ± 0.67	1.75 ± 0.09
Vec-1	14.00 ± 1.00 / 7.67 ± 0.67	1.83 ± 0.13
Vec-2	18.00 ± 1.00 / 9.67 ± 1.20	1.86 ± 0.10
Mito(−)-4	17.00 ± 0.00 / 8.67 ± 0.33	1.96 ± 0.00
Mito(−)-6	14.33 ± 0.88 / 7.33 ± 0.33	1.95 ± 0.12
MnSOD-5	9.33 ± 0.88 / 9.67 ± 0.88	0.97 ± 0.09†
MnSOD-9	9.00 ± 0.58 / 8.67 ± 1.20	1.04 ± 0.07†
MnSOD-10	11.00 ± 0.58 / 9.67 ± 0.33	1.14 ± 0.06†

*Absolute apoptotic cell number per 500 cells. Data shown in the table are the averages of three independent experiments.

†$p < 0.05$ versus KP4, $p < 0.05$ versus vec-1, $p < 0.05$ versus vec-2, $p < 0.05$ versus mito(−)-4, and $p < 0.05$ versus mito(−)-6.

lowing the irradiation. The results show 12–20% increases in NO generation in all cell types, indicating that every cell line has the ability to generate NO against oxidative stress (data not shown). In the next H/R experiments, the dye was loaded at 0, 1, 2, 3, and 6 h in air after 1 day of hypoxia treatment, and the images were acquired after 30 min of incubation. The fluorescent intensity was not changed after the H/R treatment in all cell types (Fig. 5). This result indicates that NO was not a major contributor of H/R-induced cell injury.

MnSOD suppresses H/R-induced mitochondrial ROS generation

To determine the effect of MnSOD on H/R-induced mitochondrial ROS generation, a dye sensitive to a change in mitochondrial ROS was used. For an analysis of the levels of mitochondrial ROS, we utilized the same analytic technique used for NO detection. The dye was loaded at 0, 1, 2, 3, and 6 h in air after 1 day of hypoxia treatment, and the images were acquired after 30 min of incubation. The change in the relative fluorescent intensity is shown in Fig. 6. This result shows that the relative fluorescent intensity of the dhRho was reduced in the MnSOD-transfected cells compared with the KP4, vec-1, and -2 cells, indicating that MnSOD suppresses H/R treatment-induced ROS generation in mitochondria. In addition, the change in ROS in the mito(−) cells following the H/R treatment was similar to that of the control and vector cells, indicating MnSOD lacking MTS had no effect on H/R-induced mitochondrial ROS levels.

H/R induces lipid peroxidation

To determine if changes of mitochondrial ROS generation are accompanied by an increase in lipid peroxidation products, the levels of HNE-modified proteins were evaluated by immunohistochemical staining. Preliminary experiments showed that there was no significant change in HNE-modified protein-staining intensity among all cell types using the intact cells (data not shown). The change in the relative HNE-modified protein-staining intensity in each cell line, which was obtained at 0, 1, 2, 3, and 6 h in air after 1 day of hypoxia treatment, is shown in Fig. 7. The result shows that the relative HNE-modified protein-staining intensity was suppressed in the MnSOD-transfected cells, but not in vector alone or MnSOD lacking MTS transfected cells. These results indicate that normal MnSOD, and not MnSOD lacking MTS, suppresses the levels of the H/R treatment-induced formation of intracellular HNE-modified proteins.

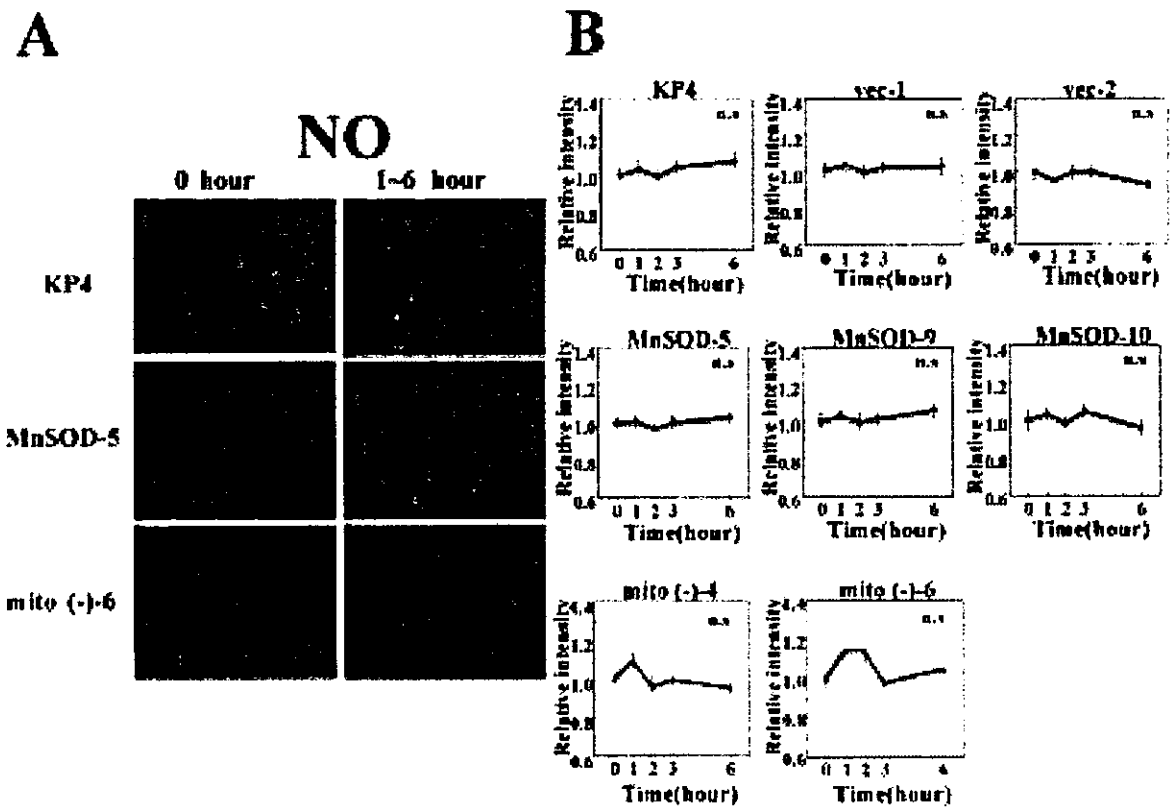

FIG. 5. Intracellular NO generation. The intracellular NO generation in each cell line at 0, 1, 2, 3, and 6 h in air after 1 day of hypoxia treatment (H/R treatment) was determined. No increase in the intracelluar NO levels was observed in all cell lines examined. The apparent increase in NO level did not achieve statical significance. **(A)** Representative photographs of cell stained with DAF. **(B)** Relative fluorescent intensity of DAF versus time (hours) in air following 1 day of hypoxia treatment (H/R treatment). n.s. not significant.

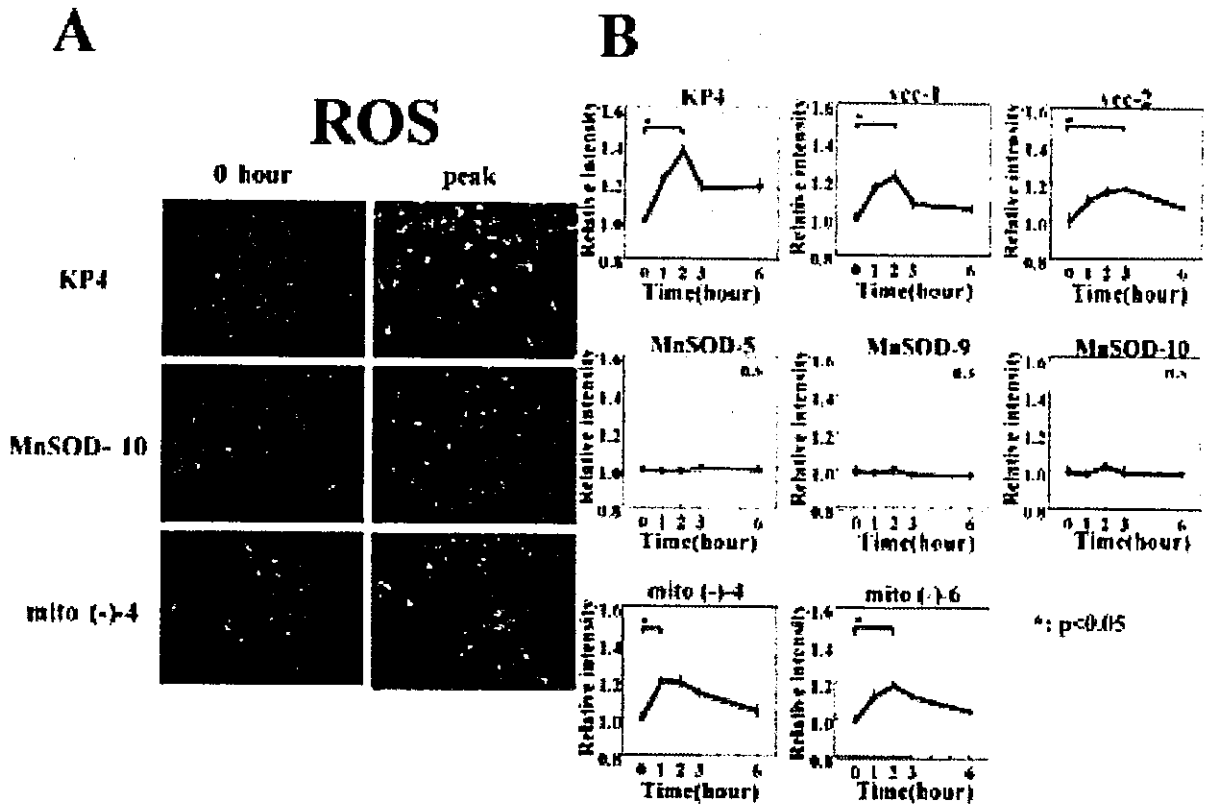

FIG. 6. Mitochondrial ROS generation. The levels of ROS in mitochondria in each cell line at 0, 1, 2, 3, and 6 h in air after 1 day of hypoxia treatment (H/R treatment) were determined. The relative fluorescent intensity of the dhRho was reduced in the MnSOD transfected cells compared with the KP4, vec-1 and -2, and mito(−) cells. **(A)** Representative images of cells examined for dhRho, at 0 h or at the peak times. **(B)** Relative fluorescent intensity of dhRho versus time (hours) in air following 1 day of hypoxia treatment (H/R treatment). n.s, not significant; $*p < 0.05$.

Correlation between mitochondrial ROS, intracellular lipid peroxidation products, and cell death

To understand better the relationship between mitochondrial ROS, intracellular lipid peroxidation, and cell death, we used a scattergram to plot (a) the relative apoptotic index against the relative dhRho (ROS) staining intensity, (b) the relative apoptotic index against the relative HNE-modified protein-staining intensity, and (c) the relative HNE-modified protein-staining intensity against the relative ROS staining intensity, and then analyzed the data using linear regression analysis. Figure 8A shows a linear-regression analysis of the relative apoptotic index against the relative mitochondrial ROS staining intensity ($r = 0.818$, $p = 0.018$). Figure 8B shows a linear-regression analysis of the relative apoptotic index versus the relative HNE-modified protein-staining intensity ($r = 0.933$, $p = 0.018$). These results show a strong positive correlation between the mitochondrial ROS, the intracellular lipid peroxidation products, and apoptosis. Figure 8C illustrates a linear-regression analysis of the relative ROS staining intensity versus the HNE-modified protein-staining intensity ($r = -0.856$, $p = 0.020$), indicating a correlation between the relative ROS staining intensity and that of HNE-modified protein adducts. Thus, intracellular mitochondrial ROS staining intensity and relative HNE-modified protein-staining intensity have a strong correlation with apoptosis, and there is a strong correlation with mitochondrial ROS staining intensity and HNE-modified protein-staining intensity.

Localization of MnSOD, MnSOD lacking MTS, and MTS signal only in KP4 cells

To examine localization of MnSOD, MnSOD lacking MTS [MnSOD mito(−)], and MTS signal alone (Mito signal), the cDNA was linked with the pEGFP vector and then transfected with KP4 cells. To localize mitochondria, the same cells were stained with MitoTracker Red CMXRos. A merged double image of GFP and MitoTracker was made to verify coexistence of MnSOD, MnSOD lacking MTS, or MTS alone in mitochondria. Figure 9 shows that MnSOD was localized in mitochondria, as shown by the color yellow (green plus red) in the double image of pEGFP and Mitotracker. A similar image was taken for MTS alone (Mito signal) in the double image, where a yellow color is clearly shown. However, for MTS-lacking MnSOD [MnSOD mito(−)], only a few yellow color regions can be seen in the double color picture, indicating the most of the MnSOD lacking MTS was localized in cytosol, although the fluorescent intensity of pEGFP in the image is unclear or obscure in the cytosol.

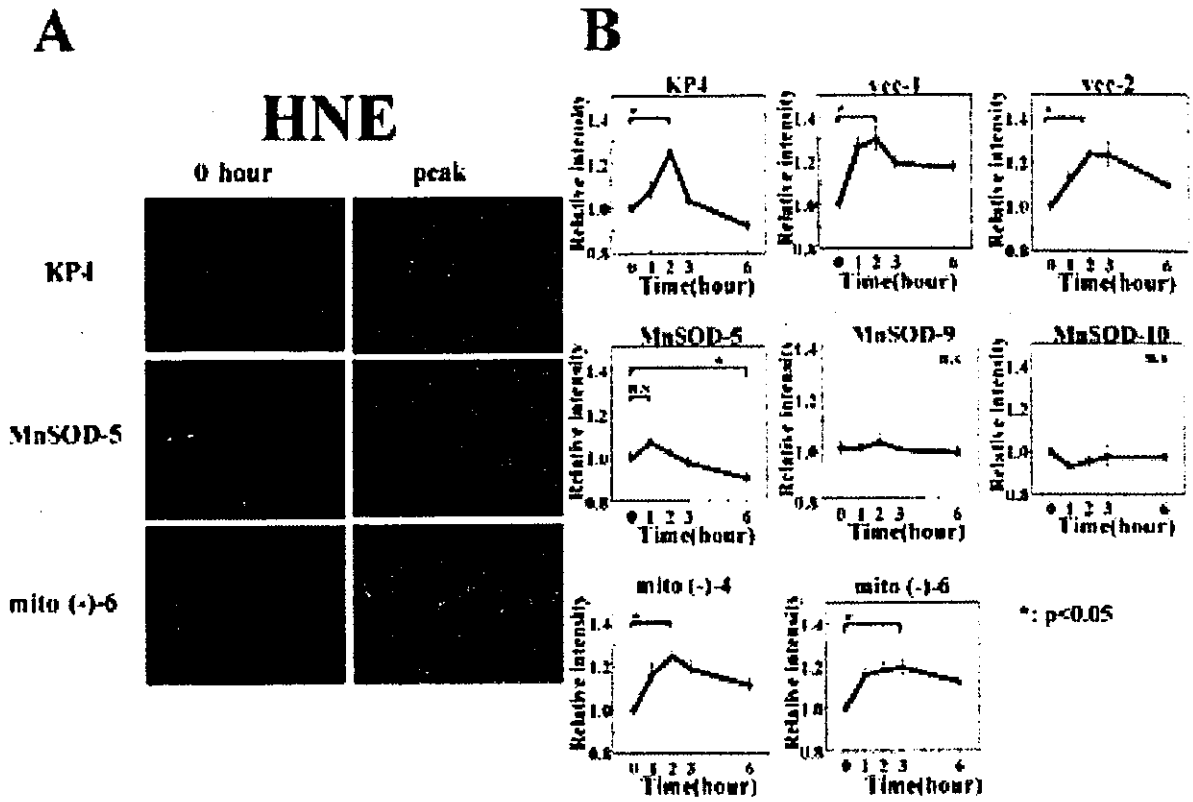

FIG. 7. Intracellular HNE adducts. The intracellular levels of HNE protein adducts in each cell line at 0, 1, 2, 3, and 6 h in air after 1 day of hypoxia treatment (H/R treatment) were determined. **(A)** Representative photographs of cell staining with an antibody against HNE protein adducts at 0 h or peak hours. **(B)** Relative fluorescent intensity of HNE protein adducts versus time (hours) in air following 1 day of hypoxia treatment (H/R treatment). n.s, not significant; $*p < 0.05$.

DISCUSSION

Using a human pancreatic tumor cell line, KP4, we first examined the effects of H/R on ROS production, lipid peroxidation, and cellular viability following 1 day of hypoxia and subsequent exposure to air. The results show that H/R increased ROS, lipid peroxidation, and apoptosis, although the apoptosis frequency was small. In this study, we investigated whether an enhanced expression of mitochondrial MnSOD, a superoxide-scavenging enzyme, can protect cells against H/R.

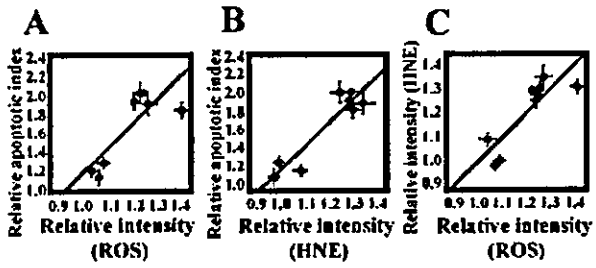

FIG. 8. Correlation between mitochondrial ROS, intracellular lipid peroxidation protein adducts, and cell death. (A) Linear-regression analysis showing the relationship between the relative apoptosis index and the relative dhRho staining intensity (mitochondrial ROS) after H/R treatment ($r = 0.818, p = 0.018$). **(B)** Relationship between the relative apoptosis index and the relative HNE protein-adducts staining intensity (intracellular lipid peroxidation products) ($r = 0.933, p = 0.018$). **(C)** Relationship between the relative dhRho staining intensity and the relative HNE protein adducts staining ($r = -0.856, p = 0.020$). Mitochondrial ROS, intracellular lipid peroxidation products, and apoptosis have a strong correlation with each other.

We found that H/R-produced apoptosis is suppressed by MnSOD, but not by mito(−) MnSOD, which is not located in the mitochondria. These results signify the importance of mitochondrial localization of MnSOD. It has been shown that adenoviral gene transfer with MnSOD is effective in reducing the extent of *in vivo* I/R injury in the rat heart (1) and in mouse liver (50), but expression of copper/zinc SOD (Cu/ZnSOD) did not function in protection in the mouse liver model (50). Given the fact that the MnSOD and Cu/ZnSOD used in these studies were mainly expressed in the mitochondria and cytosol, respectively, these results are consistent with our results. Our results further indicate that not only is active MnSOD important, but also it must be located in the mitochondria for the observed protection.

The reaction between superoxide radicals and NO to form peroxynitrite is a subject under considerable study. Superoxide radicals can react at diffusion rates with NO to form peroxynitrite, a potent biological oxidant. In this study, however, we could not find evidence of further NO induction by hypoxia treatment. This is not surprising, because oxygen is an essential substrate for NO synthesis. Our results are also consistent with various other reports that indicate that hypoxia

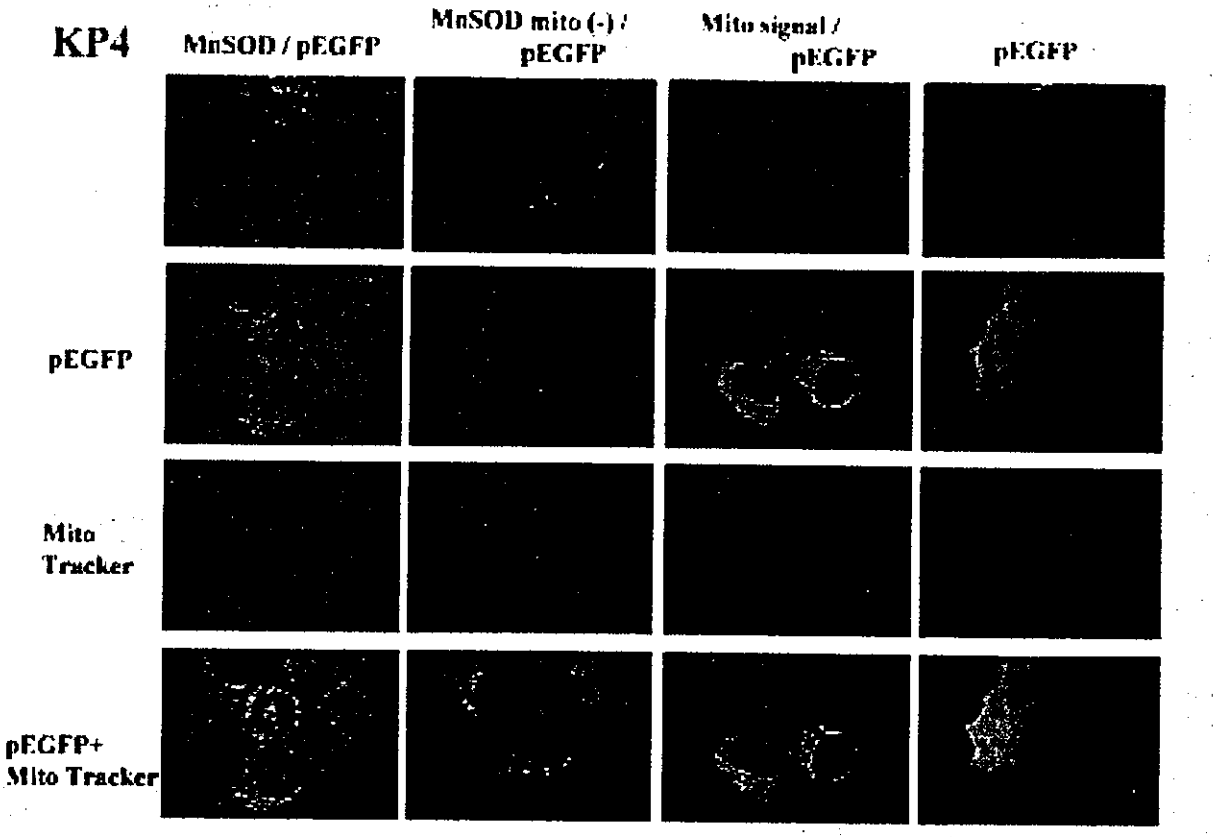

FIG. 9. Localization of MnSOD, MnSOD lacking MTS, and MTS alone in KP4 cells. Localization of full-length MnSOD, MnSOD lacking MTS [MnSOD mito (−)], and MTS signal alone (Mito signal) is shown. GFP was visualized using the pEGFP transfection sytem. To locate mitochondria, the same cells were stained with MitoTracker Red CMXRos. Merged double images of GFP and MitoTracker were made to identify MnSOD in mitochondria. MnSOD was localized in mitochondria, as shown by the yellow color (green plus red) in the double image of pEGFP and MitoTracker. A similar image was taken for MTS alone (Mito signal) in the double image, where a yellow color is clearly shown. However, for MTS lacking MnSOD [MnSOD mito (−)], only a few yellow color regions can be seen in the double color picture, indicating that most of the MnSOD lacking MTS was localized in cytosol, although the fluorescent intensity of pEGFP is unclear or obscure in cytosol in the picture.

limits NO synthesis even when NO synthase is overexpressed (for review, see 19). As ROS are increased without a concurrent increase in NO production in the H/R model, it is likely that the observed increase in HNE-modified proteins is mediated via hydroxyl radical generation. The finding that increased expression of MnSOD abolished the increased levels of HNE-modified proteins under H/R further supports this possibility.

Our results indicating that only MnSOD and not mito(−) transfectants suppress the formation of HNE-modified proteins suggest that superoxide production in the mitochondria is important for the production of HNE-modified proteins under conditions of H/R. Our results further indicate that the localization of active MnSOD in the mitochondrion is important for the suppression of ROS production and subsequent formation of HNE protein adducts. These results suggest that H/R-induced apoptosis is linked to the production of ROS and its toxic products.

Mitochondrial damage and the role of mitochondria in apoptosis are well established in various pathological conditions. However, it is largely unknown whether mitochondria are the sources or targets in such apoptosis events. Our results suggest that induction of oxidative injury in mitochondria is an upstream event leading to apoptosis in H/R-induced cell death.

Endogenous MnSOD is a nuclear-encoded protein that is cotranslationally transported into mitochondria where the signal peptide is removed and Mn is inserted to produce active proteins. The role of MnSOD in protecting against oxidative stress-mediated cell death has been demonstrated in organisms ranging from bacteria to mammals. In all studies reported thus far, it has been assumed that the effect of MnSOD is due to its location in mitochondria. However, the question remains to be investigated as to whether enzyme localized outside mitochondria has any protective effect. Our results reported here clearly demonstrate that expression of active MnSOD outside mitochondria was not effective. Although it is unclear how MnSOD located outside mitochondria acquires its Mn and proper conformation for its activity, our results from activity assay, mRNA RT-PCR assay, apoptosis observation, and colocalization studies (Table 1, Figs. 2, 4, and 9) provide strong support that active MnSOD outside mitochondria is not effective in protecting against H/R-induced apoptosis. Our GFP vector images (Fig. 9) show that

only small amounts of transfectants of MnSOD mito(−) are found in mitochondria. The distribution of GFP outside mitochondria of the MnSOD and Mito signal alone may indicate that the intensity of MnSOD lacking MTS was low because of a wide dispersion over cytosol. Although our finding that the MnSOD construct lacking MTS expresses active MnSOD protein outside mitochondria is unexpected; this phenomenon has been observed for other antioxidant enzymes as well. For example, Tamura *et al.*(37) demonstrated a much greater enhancement of cellular resistance to oxidant challenge by CHO cells by stable transfection with leader sequence of glutathione reductase (GR) cDNA than they observed in a construct lacking the MTS, which produced comparable increases in the total cellular GR activities, but did not increase mitochondrial GR activities (29, 37, 38). Arai *et al.* (2) demonstrated the effect of phospholipid hydroperoxide glutathione peroxidase, which is naturally synthesized as a long form (the L-form; 23 kDa) and a short form (the S-form; 20 kDa). The long form contains a mitochondrial targeting leader sequence, whereas the short form lacks the leader sequence. Cells transfected with the L-form containing vector were more resistant against oxidative stress, including potassium cyanide, rotenone (chemical hypoxia), and exogenous *tert*-butyl hydroperoxide oxidant injuries, compared with those cells transfected with the S-form containing vector (2). Wong (46) demonstrated that MnSOD without the mitochondrial leading targeting signal failed to protect against radiation, whereas the reduction of normal cytosolic Cu/ZnSOD or normally extracellularly expressed SOD to mitochondria with MTS resulted in protection against radiation. These results suggest that MnSOD, which is located in cytosol, does not function to prevent against H/R treatment-induced oxidative damage and cell death, and only when the enzyme is located in mitochondria does MnSOD have a function. Taken together, these data support the critical role of mitochondria localization of antioxidant enzymes for the protection against cellular injury from outside stress initiated in the mitochondrion.

In summary, the findings shown in study indicated that (a) H/R induced increased mitochondrial ROS production, lipid peroxidation protein-adducts, and subsequent apoptosis; (b) these processes were suppressed by active MnSOD in the mitochondria but not in the cytosol even when the MnSOD is active; and (c) the results support the overall hypothesis depicted in Fig. 10 showing that H/R triggers mitochondrial ROS production and generation of lipid peroxidation products, and subsequently accelerates cell death and its inhibition by MnSOD.

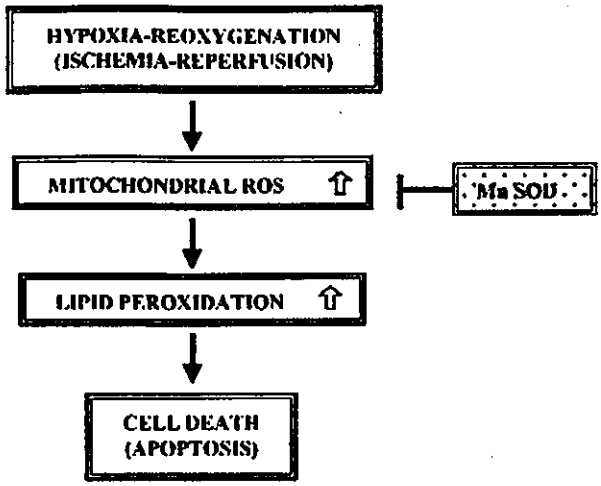

FIG. 10. Schematic diagram of a hypothesis on how ROS generation and lipid peroxidation products affect cell death (apoptosis) and its prevention by MnSOD after H/R treatment.

ABBREVIATIONS

Cu/ZnSOD, copper/zinc superoxide dismutase; DAF, diaminofluorescein; DAF-FM DA, diaminofluorescein-FM diacetate; dhRho, dihydrorhodamine 123; DMEM, Dulbecco's modified Eagle medium; GFP, green fluorescent protein; GR, glutathione reductase; HNE, 4-hydroxy-2-nonenal; H/R, hypoxia followed by reoxygenation; I/R, ischemia/reperfusion; mito(−), lacking MTS; mito(−)-, MTS lacking MnSOD transfected cell clone; MnSOD, manganese superoxide dismutase (EC 1.15.1.1); MnSOD-, MnSOD transfected cell clone; MTS, mitochondrial targeting signal; NO, nitric oxide; PBS, phosphate-buffered saline; ROS, reactive oxygen species; SOD, superoxide dismutase; vec-, vector alone transfected cell clone.

ACKNOWLEDGMENTS

The authors wish to thank Dr. Makoto Akashi (NIRS) for MnSOD cDNA, and Ms Chizuru Yamaguchi and Dr. Yoichiro Iwashita for technical assistance. This study was partially supported by "Ground Research Announcement for Space Utilization" promoted by Japan Space Forum, and The Nuclear Cross-Over Research Study, Grant-in Aid for Scientific Research (C) (2) #10671786, #12671844, #14207078, and #15659451 of Ministry of Education, Culture, Sports, Science and Technology, Japan.

REFERENCES

1. Abunasra HJ, Smolenski RT, Morrison K, Yap J, Sheppard MN, O'Brien T, Suzuki K, Jayakumar J, and Yacoub MH. Efficacy of adenoviral gene transfer with manganese superoxide dismutase and endothelial nitric oxide synthase in reducing ischemia and reperfusion injury. *Eur J Cardiothorac Surg* 20: 153–158, 2001.
2. Arai M, Imai H, Koumura T, Yoshida M, Emoto K, Umeda M, Chiba N and Nakagawa Y. Mitochondrial phospholipid hydroperoxide glutathione peroxidase plays a major role in preventing oxidative injury to cells. *J Biol Chem* 274: 4924–4933, 1999.
3. Beauchamp C and Fridovich I. Superoxide dismutase: improved assays and an assay applicable to acrylamide gels. *Anal Biochem* 44: 276–287, 1971.
4. Bienvenu P, Caron L, Gasparutto D, and Kergonou JF. Assessing and counteracting the prooxidant effects of anticancer drugs. *EXS* 62: 257–265, 1992.

5. Boveris A and Cadenas E. Mitochondrial production of superoxide anions and its relationship to the antimycin insensitive respiration. *FEBS Lett* 1: 311–314, 1975.
6. Brown JM. Evidence for acutely hypoxic cells in mouse tumours, and a possible mechanism of reoxygenation. *Br J Radiol* 52: 650–656, 1979.
7. Brown JM. The hypoxic cell: a target for selective cancer therapy—eighteenth Bruce F. Cain Memorial Award lecture. *Cancer Res* 59: 5863–5870, 1999.
8. Carlioz A and Touati D. Isolation of superoxide dismutase mutants in *Escherichia coli:* is superoxide dismutase necessary for aerobic life? *EMBO J* 5: 623–630, 1986.
9. Chomczynski P and Sacchi N. Single-step method of RNA isolation by acid guanidinium thiocyanate–phenol–chloroform extraction. *Anal Biochem* 162: 156–159, 1987.
10. Engelhardt JF. Redox-mediated gene therapies for environmental injury: approaches and concepts. *Antioxid Redox Signal* 1: 5–27, 1999.
11. Farr SB, D'Ari R, and Touati D. Oxygen-dependent mutagenesis in *Escherichia coli* lacking superoxide dismutase. *Proc Natl Acad Sci USA* 83: 8268–8272, 1986.
12. Halliwell B and Gutteridge JMC. Free radicals, other reactive species and disease. In: *Free Radicals in Biology and Medicine,* 3rd edit., edited by Halliwell B and Gutteridge JMC. Oxford, U.K.: Oxford University Press, 1999, pp.617–783.
13. Hirose K, Longo DL, Oppenheim JJ, and Matsushima K. Overexpression of mitochondrial manganese superoxide dismutase promotes the survival of tumor cells exposed to interleukin-1, tumor necrosis factor, selected anticancer drugs, and ionizing radiation. *FASEB J* 7: 361–368, 1993.
14. Ho YS and Crapo JD Isolation and characterization of complementary DNAs encoding human manganese-containing superoxide dismutase. *FEBS Lett* 229: 256–260, 1988.
15. Kiningham KK, Oberley TD, Lin S, Mattingly CA, and St Clair DK. Overexpression of manganese superoxide dismutase protects against mitochondrial-initiated poly(ADP-ribose) polymerase-mediated cell death. *FASEB J* 13: 1601–1610, 1999.
16. Knisely JP and Rockwell S. Importance of hypoxia in the biology and treatment of brain tumors. *Neuroimaging Clin NAm* 12: 526–536, 2002.
17. Kojima H, Nakatsubo N, Kikuchi K, Kawahara S, Kirino Y, Nagoshi H, Hirata Y, and Nagano T. Detection and imaging of nitric oxide with novel fluorescent indicators: diaminofluoresceins. *Anal Chem* 70: 2446–2453, 1998.
18. Lebovitz RM, Zhang H, Vogel H, Cartwright J Jr, Dionne L, Lu N, Huang S, and Matzuk MM. Neurodegeneration, myocardial injury, and perinatal death in mitochondrial superoxide dismutase deficient mice. *Proc Natl Acad Sci U S A* 93: 9782–9787, 1996.
19. Le Cras TD and McMurtry IF. Nitric oxide production in the hypoxic lung. *Am J Physiol Lung Cell Mol Physiol* 280: L575–L582, 2001.
20. Lee JM, Zipfel GJ, and Choi DW. The changing landscape of ischaemic brain injury mechanisms. *Nature* 399 (6738 Suppl): A7–A14, 1999.
21. Li Y, Huang T-T, Carlson EJ, Melov S, Ursell PC, Olson JL, Noble LJ, Yoshimura MP, Berger C, Chan PH, Wallace DC, and Epstein CJ. Dilated cardiomyopathy and neonatal lethality in mutant mice lacking manganese superoxide dismutase. *Nat Genet* 11: 376–381, 1995.
22. Lithgow T. Targeting of proteins to mitochondria. *FEBS Lett* 476: 22–26, 2000.
23. Majima HJ, Oberley TD, Furukawa K, Mattson MP, Yen HC, Szweda LI, and St. Clair DK. Prevention of mitochondrial injury by manganese superoxide dismutase reveals a primary mechanism for alkaline-induced cell death. *J Biol Chem* 273: 8217–8224, 1998.
24. Mattson MP. Apoptosis in neurodegenerative disorders. *Nat Rev Mol Cell Biol* 1: 120–129, 2000.
25. Mattson MP, Duan W, Pedersen WA, and Culmsee C. Neurodegenerative disorders and ischemic brain diseases. *Apoptosis* 6: 69–81, 2001.
26. Mihara T and Onuma T. Cytoplasmic chaperons in precursor targeting to mitochondria: the role of MSF and hsp70. *Trends Cell Biol* 6: 104–108, 1996.
27. Motoori S, Majima HJ, Ebara M, Kato H, Hirai F, Kakinuma S, Yamaguchi C, Ozawa T, Nagano T, Tsujii H, and Saisho H. Overexpression of mitochondrial manganese superoxide dismutase protects against radiation-induced cell death in the human hepatocellular carcinoma cell line HLE. *Cancer Res* 61: 5382–5388, 2001.
28. Nishi Y, Haji M, Takayanagi R, Iguchi H, Shimazoe T, Hirata J, and Nawata H. Establishment of characterization of PTHrP-producing human pancreatic cancer cell line. *Int J Oncol* 5: 33–39, 1994.
29. O'Donovan DJ, Katkin JP, Tamura T, Husser R, Xu X, Smith CV, and Welty SE. Gene transfer of mitochondrially targeted glutathione reductase protects H441 cells from *t*-butyl hydroperoxide-induced oxidant stresses. *Am J Respir Cell Mol Biol* 20: 256–263, 1999.
30. Riley PA. Free radicals in biology: oxidative stress and the effects of ionizing radiation. *Int J Radiat Biol* 65: 27–33, 1994.
31. Rofstad EK. Microenvironment-induced cancer metastasis. *Int J Radiat Biol* 76: 589–605, 2000.
32. St Clair DK, Oberley TD, and Ho Y-S. Overproduction of human Mn-superoxide dismutase modulates paraquat-mediated toxicity in mammalian cells. *FEBS Lett* 293: 199–203, 1991.
33. St. Clair DK, Wan XS, Oberley TD, Muse KE, and St Clair WH. Suppression of radiation-induced neoplastic transformation by overexpression of mitochondrial superoxide dismutase. *Mol Carcinog* 6: 238–242, 1992.
34. St Clair DK, Jordan JA, Wan S, and Gairola CG. Protective role of manganese superoxide dismutase against cigarette smoke-induced cytotoxicity. *J Toxicol Environ Health* 43: 239–249, 1994.
35. Sun J, Chen Y, Li M, and Ge Z. Role of antioxidant enzymes on ionizing radiation resistance. *Free Radic Biol Med* 24: 586–593, 1998.
36. Takeshige K and Minakami S. NADH- and NADPH-dependent formation of superoxide anions by bovine heart submitochondrial particles and NADH-ubiquinone reductase preparation. *Biochem J* 180: 129–135, 1979.
37. Tamura T, McMicken HW, Smith CV, and Hansen TN. Mitochondrial targeting of glutathione reductase requires a leader sequence. *Biochem Biophys Res Commun* 222: 659–663, 1996.